



Cite this: *RSC Adv.*, 2020, **10**, 2791

Design, eco-friendly synthesis, molecular modeling and anticancer evaluation of thiazol-5(4H)-ones as potential tubulin polymerization inhibitors targeting the colchicine binding site†

Abeer M. El-Naggar, ^{*a} Ibrahim H. Eissa, ^{*c} Amany Belal ^b and Amira A. El-Sayed ^a

In recent years, suppressing tubulin polymerization has been developed as a therapeutic approach for cancer treatment. Thus, new derivatives based on thiazol-5(4H)-ones have been designed and synthesized in an eco-friendly manner. The synthesized derivatives have the same essential pharmacophoric features of colchicine binding site inhibitors. The anti-proliferative activity of the new derivatives was evaluated on three human cancer cell lines (HCT-116, HepG-2, and MCF-7) using MTT assay procedure and colchicine was used as a positive control. Compounds **4f**, **5a**, **8f**, **8g**, and **8k** showed superior antiproliferative activities against the three tested cell lines with IC_{50} values ranging from 2.89 to 9.29 μ M. Further investigation for the most active cytotoxic agents as tubulin polymerization inhibitors was also performed in order to explore the mechanism of their anti-proliferative activity. Tubulin polymerization assay results were found to be comparable with the cytotoxicity results. Compounds **4f** and **5a** were the most potent tubulin polymerization inhibitors with an IC_{50} value of 9.33 and 9.52 nM, respectively. Further studies revealed the ability of **5a** to induce apoptosis and arrest cell cycle growth at the G2/M phase. Molecular docking studies were also conducted to investigate possible binding interactions between the target compounds and the tubulin heterodimer active site. From these studies, it was concluded that inhibition of tubulin polymerization yields the reported cytotoxic activity.

Received 2nd December 2019
 Accepted 7th January 2020

DOI: 10.1039/c9ra10094f
rsc.li/rsc-advances

1. Introduction

Cancer is a complex, widespread, and lethal disease. It begins when cells start to grow beyond their usual boundaries, then can invade adjoining parts of the body and spread to other organs.¹ Many of the currently available antitumor drugs are unable to differentiate between normal and neoplastic cells, and are also unable to overcome primary or secondary resistance mechanisms evolved in the tumor cells.^{2,3} Thus, there is a pressing need for new antitumor agents with high potency, and less toxicity in non-cancerous cells, that are able to act on unique targets.

Microtubules, the key components of the cytoskeleton are essential in all eukaryotic cells. Microtubules are composed of

α -tubulin and β -tubulin heterodimers arranged in the form of slender filamentous tubes that can be many micrometres long.⁴ They are highly dynamic polymers and their polymerization dynamics are tightly regulated both spatially and temporally.⁵ They are crucial in the development and maintenance of cell shape and cell division (mitosis).⁶ During mitosis process, the duplicated chromosomes of a cell are separated into two identical sets before cleavage of the cell into two daughter cells.⁷

The importance of microtubules in mitosis and cell division makes it an important target for anticancer drugs.⁸ Microtubules and their dynamics are considered targets for diverse groups of antimitotic drugs (with various tubulin-binding sites) that have been used with great success in the treatment of cancer.⁹ In view of the success of this class of drugs, it has been argued that microtubules represent the best cancer target to be identified so far, and it seems likely that drugs of this class will continue to be important chemotherapeutic agents, even as more selective approaches are developed¹⁰

The tubulin heterodimer contains at least three distinct drug binding sites: the paclitaxel (taxanes alkaloid), vinblastine (vinca alkaloid), and colchicine binding sites.¹¹ For the first two of these sites, there are many drugs in current use in clinical

^aChemistry Department, Faculty of Science, Ain Shams University, Abbassiya, Cairo, 11566, Egypt. E-mail: elsayedam@sci.asu.edu.eg

^bMedicinal Chemistry Department, Faculty of Pharmacy, Beni-Suef University, Beni-Suef 62415, Egypt

^cPharmaceutical Medicinal Chemistry & Drug Design Department, Faculty of Pharmacy (Boys), Al-Azhar University, Cairo, 11884, Egypt. E-mail: Ibrahimeissa@azhar.edu.eg

† Electronic supplementary information (ESI) available. See DOI: [10.1039/c9ra10094f](https://doi.org/10.1039/c9ra10094f)



oncology.^{12,13} All the marketed tubulin inhibitors bind to the paclitaxel and vinblastine binding sites are highly potent but the clinical use is limited for several reasons: (i) they are prone to develop multi-drug resistance, (ii) they are highly lipophilic and have to be solubilized by surfactants which can cause hypersensitivity reactions in patients, (iii) they have to be administered intravenously due to poor water solubility which is not convenient for patients and may lead to poor patient compliance.¹⁴

Tubulin inhibitors that bind to the colchicine binding site can largely overcome the above drawbacks and have therapeutic advantages over taxanes and vinca alkaloids. For example, they can be administered orally owing to the higher water solubility, they do not require surfactants for solubilization, thus are devoid of surfactant-induced hypersensitivity reaction. More importantly they are less prone to develop multi-drug resistance. Therefore, tubulin inhibitors that bind to colchicine binding site have received extraordinary attention in the last ten years.¹⁵

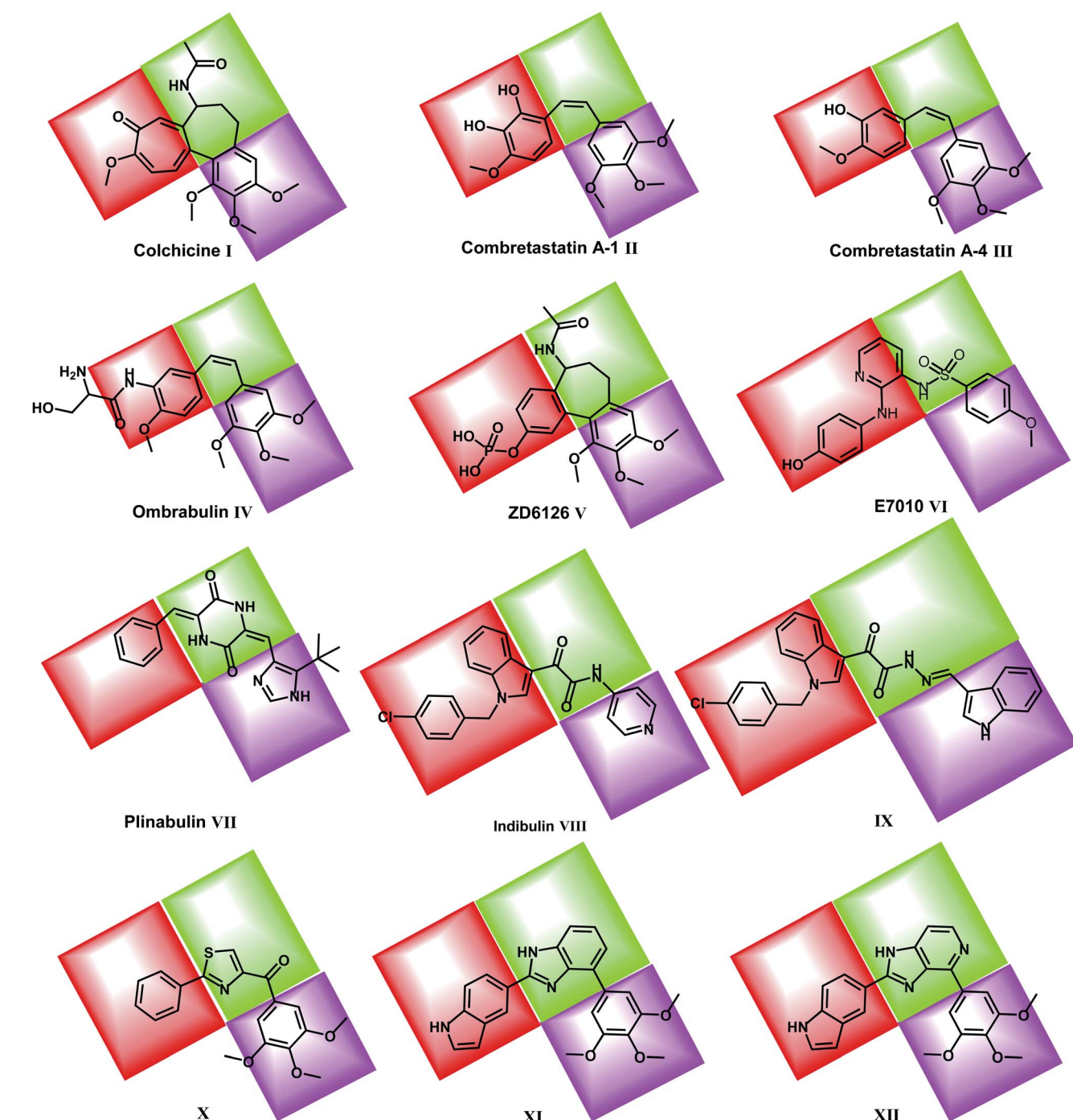


Fig. 1 Reported colchicine binding site inhibitors.



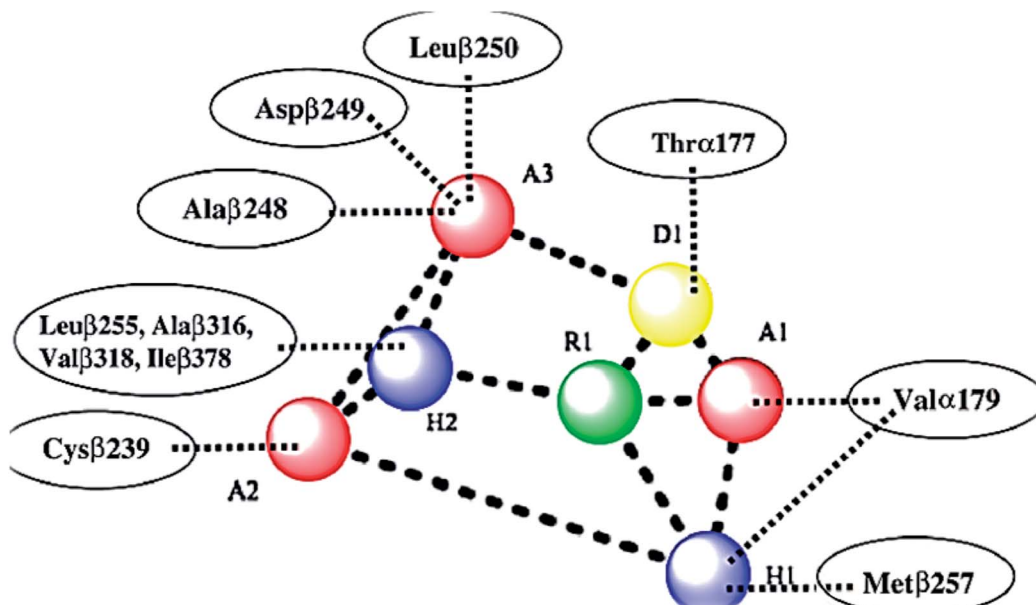


Fig. 2 Seven pharmacophoric features: three hydrogen bond acceptors (A1, A2 & A3), one hydrogen bond donor (D1), two hydrophobic centers (H1 & H2), and one planar group (R1) (based on ref. 14 and 32).

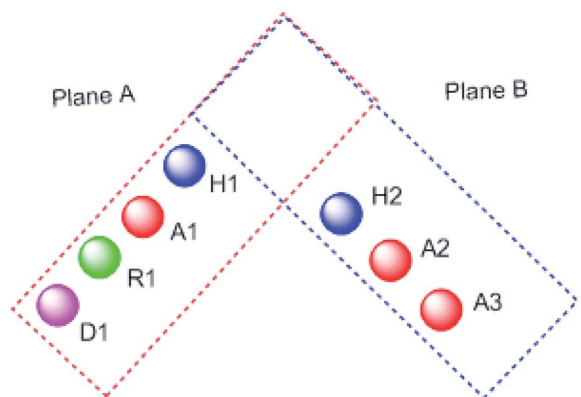


Fig. 3 The pharmacophoric model with two planes: plane A (red) points A1, D1, H1 and R1, Plane B (blue) consists of points A2, A3, and H2, and (based on ref. 32).

Colchicine binding site inhibitors (CBSIs) exert their biological effects by inhibiting tubulin assembly and suppressing microtubule formation.¹⁴ Colchicine **I** itself binds to tubulin very tightly, but neither colchicine nor compounds that bind to the colchicine binding site on tubulin have yet found significant use in cancer treatment.¹⁶ Combretastatin A-1 (CA-1) **II** and combretastatin A-4 (CA-4) **III** are two combretastatin analogs, both showed similar microtubule inhibitory activity but have limited water solubility.¹⁷ In order to improve the water solubility, both compounds were prepared as prodrugs of monosodium phosphate salt, and they can be transformed into the active components CA-1 and CA-4 *in vivo*.^{18,19} In phase II clinical trial, CA-4P showed no bone marrow toxicity, stomatitis, and hair loss.²⁰ Ombrabulin **IV** is another CA-4 analog which has better solubility, oral bioavailability, improved anti-cancer activity and decreased toxicity.¹⁴

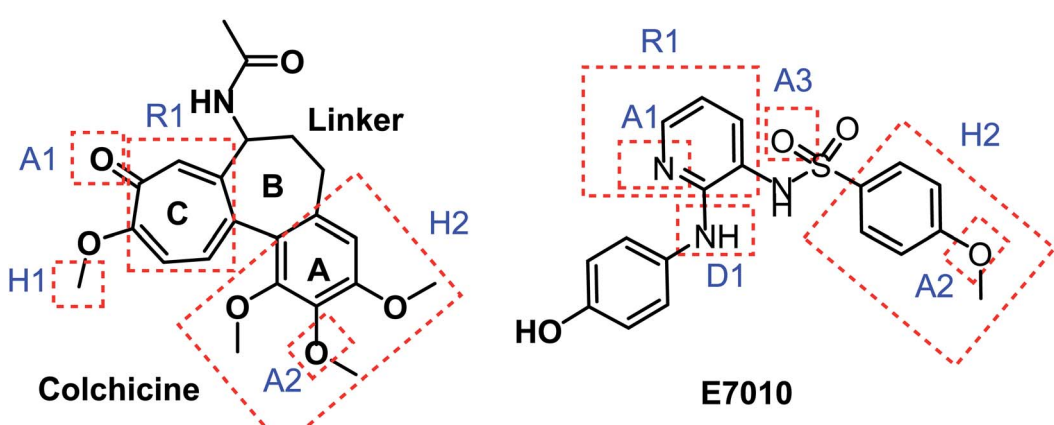


Fig. 4 Pharmacophoric points of colchicine and E7010 as CBSIs.



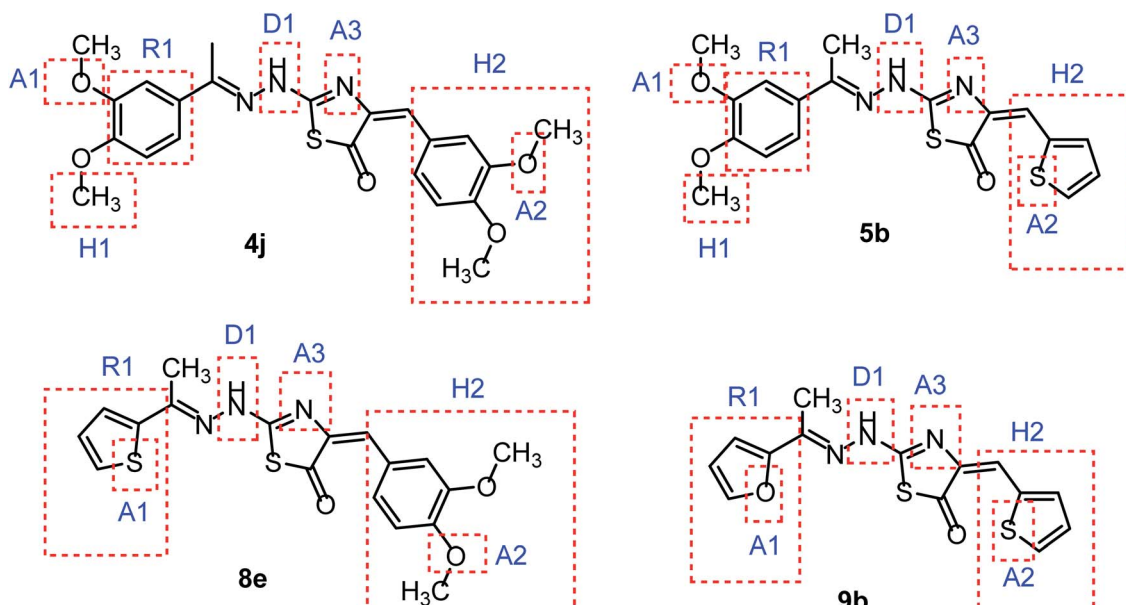


Fig. 5 Some new thiazol-5(4H)-ones having the same essential pharmacophoric features of the reported CBSIs.

ZD6126 **V** is a NAC (*N*-acetylcolchicinol) phosphate prodrug which showed microtubule inhibitory activity *in vivo*. Moreover, it showed no obvious neurotoxicity and displayed good antitumor activity.^{21,22} E7010 **VI** is an orally bioavailable sulfonamide that inhibits tubulin polymerization by binding to the colchicine binding site. It exhibited a broad spectrum of antitumor activity *in vitro* and *in vivo*.²³

Plinabulin **VII** is in a world-wide Phase III clinical trial for non-small cell lung cancer.²⁴ Plinabulin blocks the polymerization of tubulin in a unique manner, resulting in multi-factorial effects including an enhanced immune-oncology

response,²⁵ activation of the JNK pathway and disruption of the tumor blood supply.²⁶

Indibulin **VIII** has shown promising anticancer activity with a minimal neurotoxicity in preclinical animal studies and in Phase I clinical trials for cancer chemotherapy.²⁷ The antitumor activity of indibulin is believed to be primarily related to its effects on microtubules.²⁸

Recently, many molecules (e.g. compounds **IX**, **X**, **XI** & **XII**) interacting with the colchicine binding site have been designed and synthesized with significant structural diversity. These

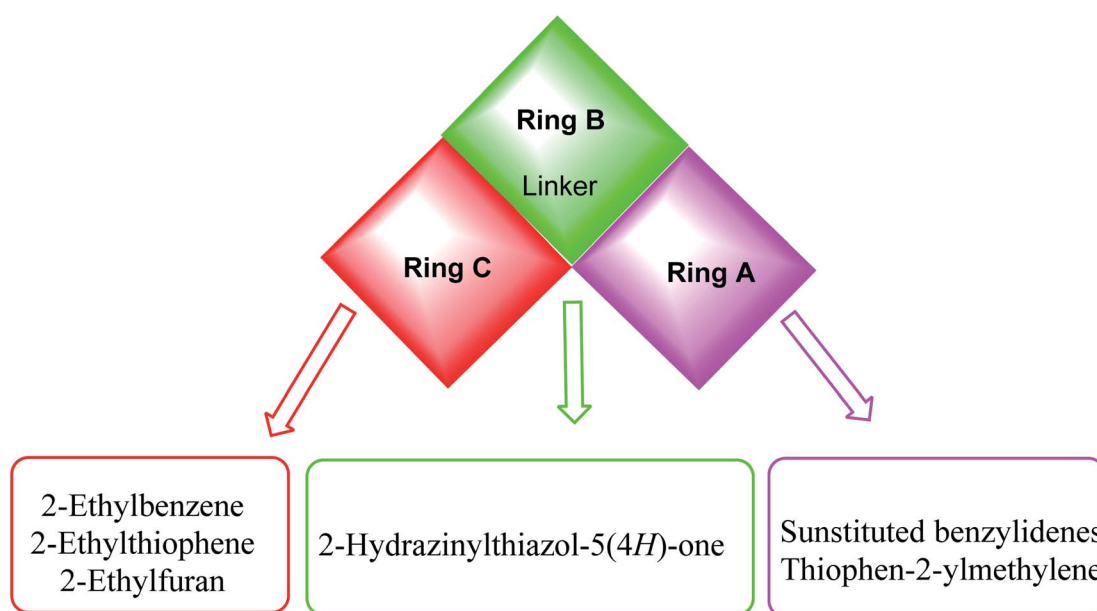


Fig. 6 Summary for the possible modifications of CBSIs.



compounds were modified and tested in order to find a highly potent, low toxicity agent for treatment of cancers^{29,30} (Fig. 1).

In the present work, our research group synthesized a series of thiazol-5(4*H*)-ones having the same pharmacophoric features of CBSIs and targeting the colchicine binding site, to examine their effect as anticancer agents with potential inhibitory effect on tubulin assembly.

1.1. Rational drug design

The colchicine binding site is positioned at the interface between the α and β subunits of the tubulin protein, with the major part of it buried in the β subunit and lined by the helices 7 and 8. The cavity, which is funnel shaped, has a volume of

about 600 \AA^3 and opens up towards the α subunit of the interface surrounded by residues Asn101 α , Thr179 α , Ala180 α , Val181 α , Thr314 β , Asn349 β , Asn350 β , and Lys352 β . The other, β subunit, end of the cavity is surrounded by residues Tyr202 β , Val238 β , Thr239 β , Cys241 β , Leu242 β , Leu248 β , Leu252 β , Leu255 β , Ile378 β , and Val318 β and forms the narrow funnel end-like part of the cavity. The predominance of hydrophobic residues confer a strong hydrophobic character to this part of the cavity. At the wider portion, the cavity is surrounded by Ala250 β , Asp251 β , Lys254 β , Asn258 β , Met259 β , Ala316 β , Ala317 β , Thr353 β and Ala354 β making it moderately polar/moderately hydrophobic.³¹

As shown in Fig. 2, colchicine binding site inhibitors have the following seven pharmacophoric points: three hydrogen

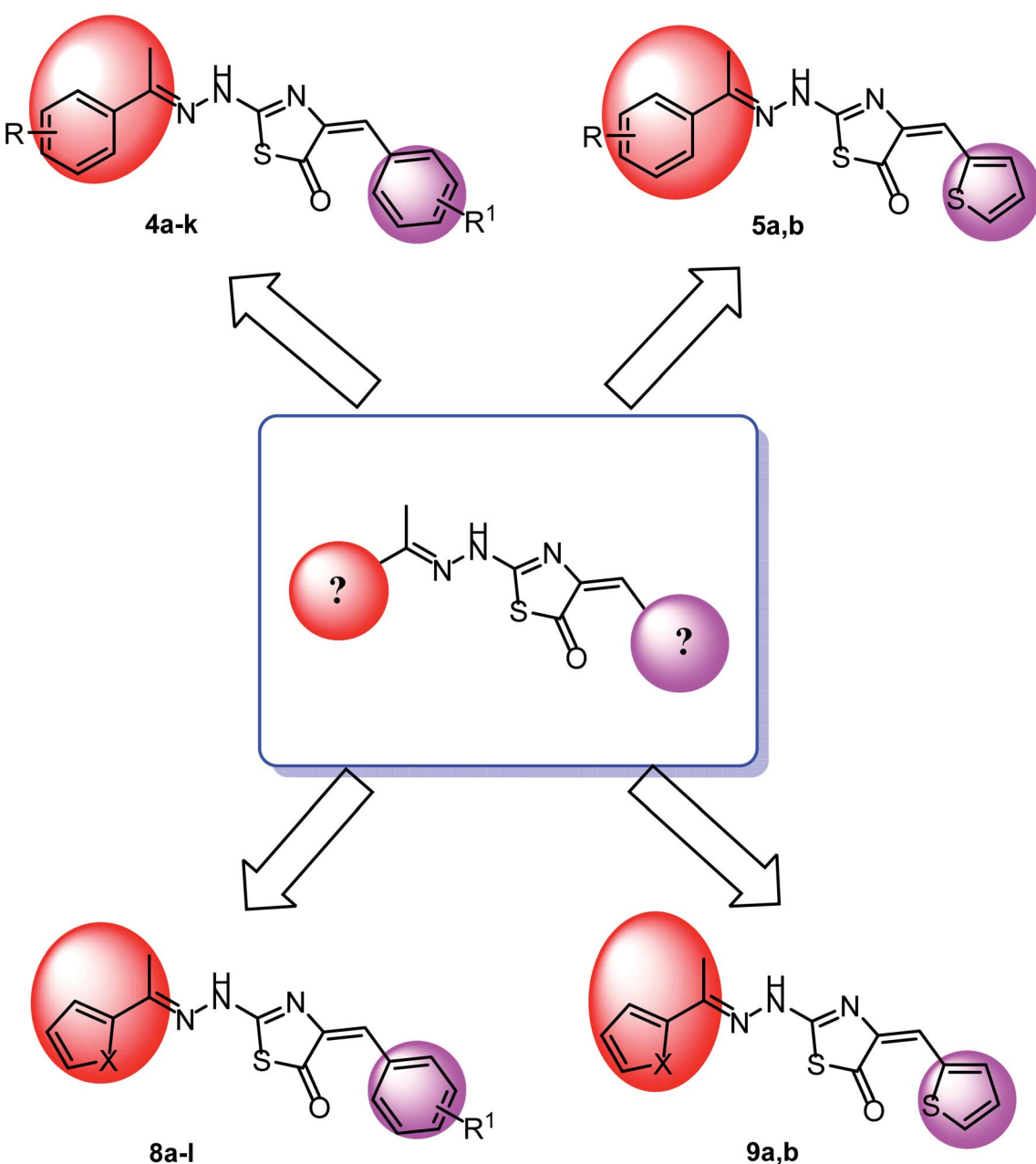


Fig. 7 Rational of molecular design of the new proposed CBSIs.



bond acceptors (A1, A2, and A3), one hydrogen bond donor (D1), two hydrophobic centers (H1 and H2) and one planar group (R1).^{14,32} Depending on these previously reported facts we can say that the molecules that will have these seven pharmacophoric features will be considered as promising tubulin inhibitors.

It is worth mentioning that, the seven pharmacophoric features can be partitioned among two planes. Features A1, D1, H1, and R1 lie in plane A, and features A2, A3, and H2 lie in plane B. Relative to one another, the two planes have a tilt of about 45° and match the shape of the colchicine site³² (Fig. 3).

Taking colchicine, as a lead compound for synthesis of the new derivatives, it is formed of three parts: ring A, ring B (linker), and ring C. Structure–activity study reveals that the A and C ring of colchicine comprise the minimal structural feature of the molecule needed for its high affinity binding to tubulin.³³ The changes to the linker region affect the cytotoxic activity of the most reported colchicine binding site inhibitors.³⁴ Fig. 4 showed the pharmacophoric points of colchicine and E7010 as representative examples of CBSIs.

In continuation for our previous work of design and synthesis of new anticancer agents,^{35–45} the main target of this work was the synthesis of new thiazol-5(4H)-ones having the same essential pharmacophoric features of the reported CBSIs (Fig. 5). The core of our molecular design rational comprised

bioisosteric modification strategies of CBSIs at three different positions.

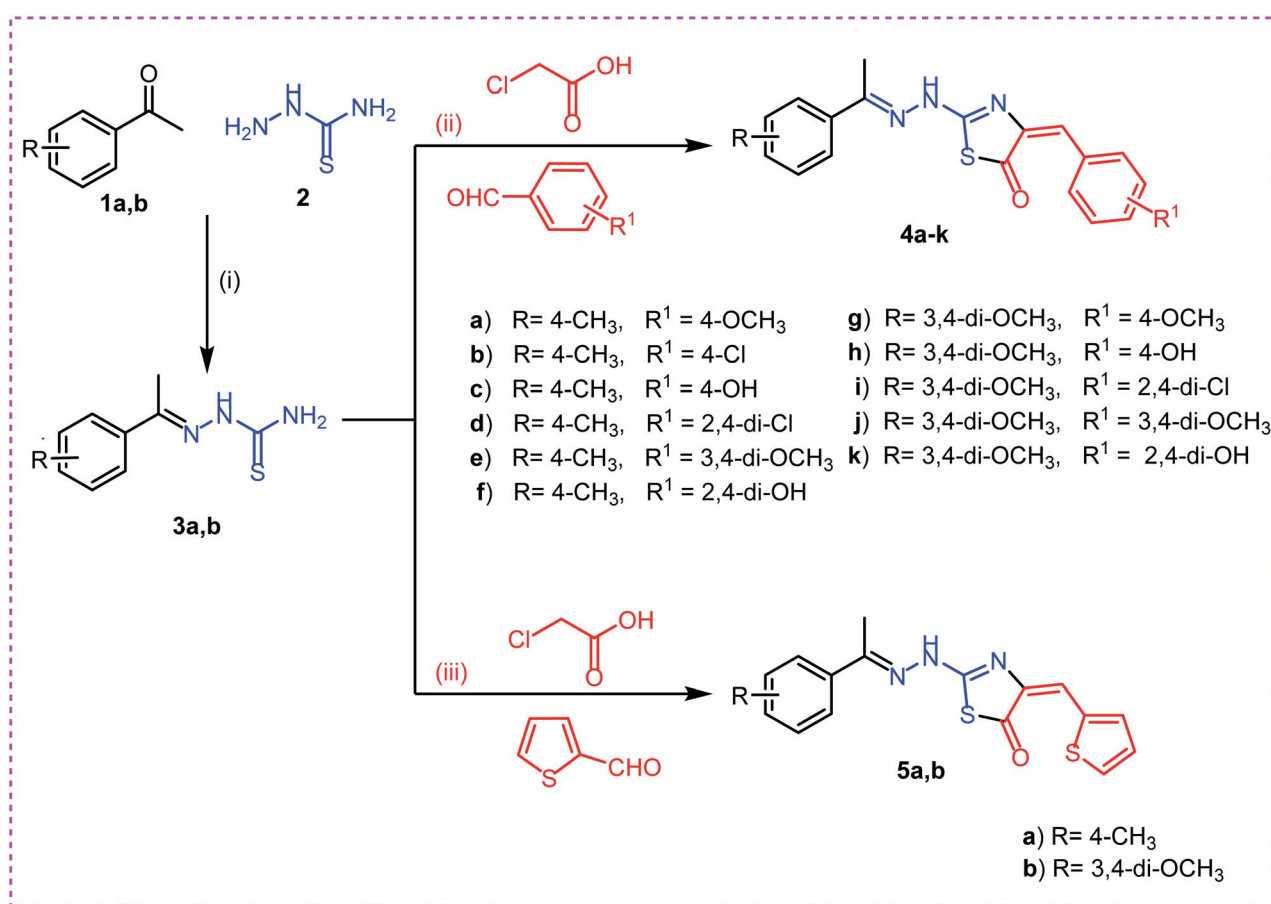
The first position was the ring A, where different substituted benzylidenes (compounds **4a–k** & **8a–l**) and thiophen-2-ylmethylene moiety (compounds **5a,b** & **9a,b**) were used as bioisosteres for ring A. The second position was the ring C, where different substituted 2-ethylbenzene moieties (compounds **4a–k** & **5a,b**), 2-ethylthiophene moiety (compounds **8a–l** & **9a**), and 2-ethylfuran moiety (compound **9b**) were used as a bioisostere for ring C. The third position was the linker region, where 2-hydrazinylthiazol-5(4H)-one moiety was used to occupy the linker region in all compounds (Fig. 6).

The wide variety of modifications enabled us to study the SAR of these compounds as effective anti-cancer agents with potential tubulin polymerization inhibitory activity which is considered as a crucial objective of our work. All modification pathways and molecular design rationale were illustrated and summarized in Fig. 7.

2. Results and discussion

2.1. Chemistry

On the bases of green considerations and in continuation of our earlier endeavors^{46–48} toward the development of eco-friendly synthetic routes for heterocyclic systems, we report herein



Scheme 1 Synthesis of target compounds **4a–k** and **5a,b**. Reagents and conditions: (i), (ii) and (iii): absolute ethanol and gl. acetic acid/reflux.



facile routes to various thiazol-5(4*H*)-one derivatives. In addition to conventional method, ultra-sound irradiation and microwave irradiation (solvent less) techniques were used in the synthesis of the new members. The reactions have been worked well in a one-pot fashion and were completed in a few minutes, with the desired products obtained in good yields.

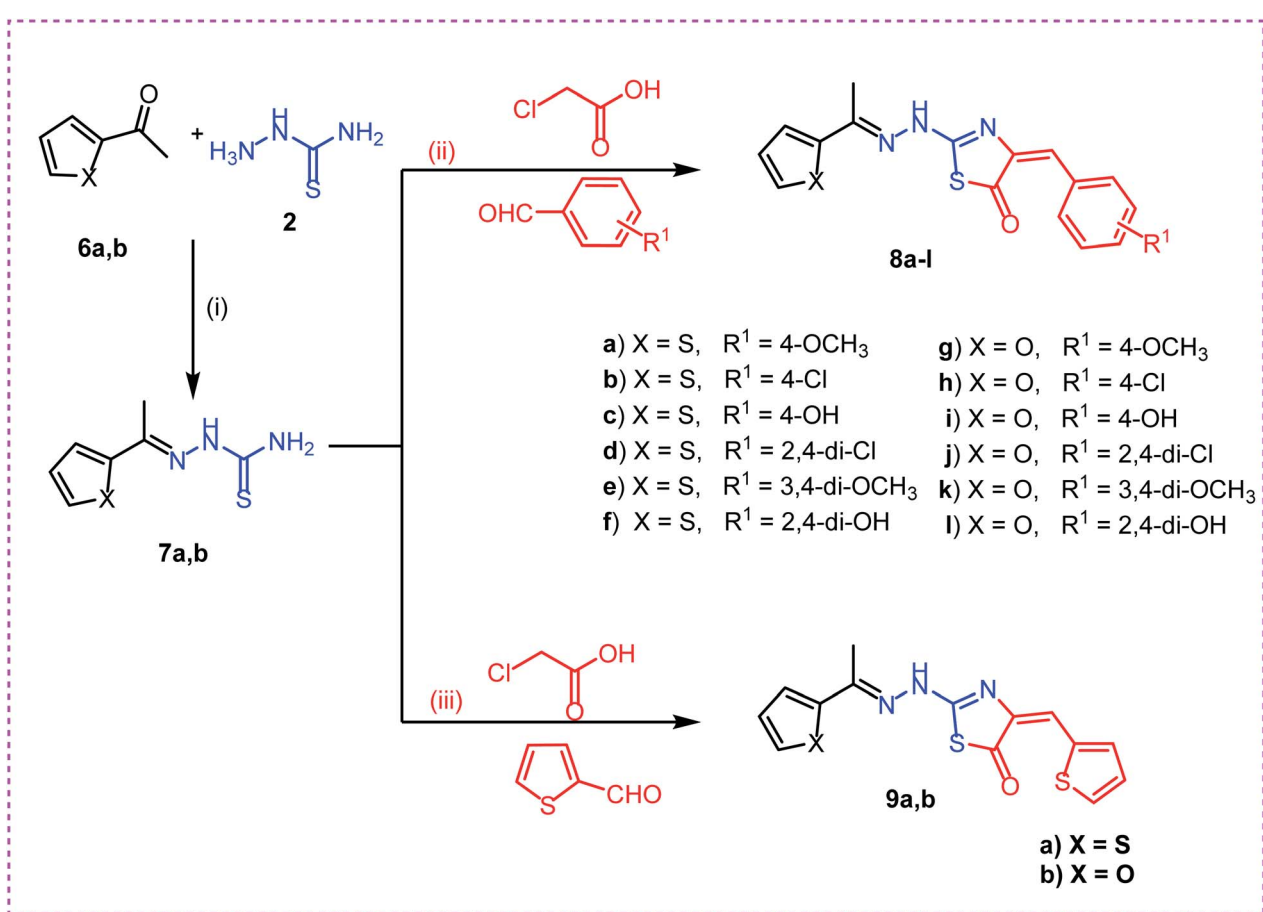
The synthetic strategies adopted to obtain the target compounds are depicted in (Schemes 1 & 2). Firstly, refluxing of aryl ketones namely, 4-methyl acetophenone **1a** and 3,4-methoxy acetophenone **1b** with thiosemicarbazide **2** in absolute ethanol with catalytic amount of glacial acetic acid afforded the key intermediates thiosemicarbazones **3a,b**. Reaction of thiosemicarbazones **3a,b** with chloroacetic acid and appropriate substituted aromatic aldehydes namely, 4-methoxy benzaldehyde, 4-chloro benzaldehyde, 4-hydroxy benzaldehyde, 2,4-dichloro benzaldehyde, 3,4-dimethoxy benzaldehyde, and 2,4-dihydroxy benzaldehyde in ethanol and catalytic amount of glacial acetic acid afforded the target compounds **4a-k**, respectively. Next, reaction of thiosemicarbazones **3a,b** with chloroacetic acid and thiophene-2-carbaldehyde in ethanol and catalytic amount of glacial acetic acid afforded the target compounds **5a,b**, respectively (Scheme 1).

Secondly, reaction of aryl ketones namely, 2-acetyl thiophene **6a** and 2-acetyl furan **6b** with thiosemicarbazide **2** in absolute

ethanol with catalytic amount of glacial acetic acid gave the corresponding thiosemicarbazones **7a,b**. Reaction of thiosemicarbazones **7a,b** with chloroacetic acid and appropriate substituted aromatic aldehydes namely, 4-methoxy benzaldehyde, 4-chloro benzaldehyde, 4-hydroxy benzaldehyde, 2,4-dichloro benzaldehyde, 3,4-dimethoxy benzaldehyde, and 2,4-dihydroxy benzaldehyde in ethanol and catalytic amount of glacial acetic acid afforded the target compounds **8a-l**, respectively. Next, reaction of thiosemicarbazones **7a,b** with chloroacetic acid and thiophene-2-carbaldehyde in ethanol and catalytic amount of glacial acetic acid afforded the target compounds **9a,b**, respectively (Scheme 2).

Finally, we repeated the two consequence steps of the reaction under both ultrasonic (in ethanol and catalytic amount of acetic acid) and microwave irradiation solvent-free conditions without isolation of the intermediates **3a,b** and **7a,b**. The reaction mixture afforded the same products with increased yield and shortage in the reaction time under ultrasonic method. Surprisingly, the yield was increased dramatically to 92%.

The structures of the synthesized compounds were established based on spectral data. The IR spectra of compound **3a,b** showed the presence of NH₂ and NH absorptions at a range of 3376–3151 cm⁻¹. The ¹H NMR spectra of compounds **3a,b** exhibited singlet signals of methyl group at 2.32 ppm, singlet



Scheme 2 Synthesis of target compounds **8a-l** and **9a,b**. Reagents and conditions: (i), (ii) and (iii): absolute ethanol and gl. acetic acid/reflux.



Table 1 *In vitro* anti-proliferative activities of the tested compounds and *in vitro* tubulin polymerization inhibition

Comp.	IC ₅₀ ^a (μM)			IC ₅₀ (nM) Tubulin polymerization inhibition
	HCT-116	HepG-2	MCF-7	
3a	NA ^b	NA ^b	NA ^b	NT ^c
3b	17.33 ± 1.4	12.91 ± 0.4	22.38 ± 1.0	44.47 ± 2.3
4a	45.61 ± 3.5	34.04 ± 30.9	NA ^b	NT ^c
4b	18.17 ± 1.3	11.14 ± 0.1	22.41 ± 1.0	NT ^c
4c	38.45 ± 2.5	35.20 ± 0.8	41.80 ± 1.2	NT ^c
4d	10.64 ± 0.4	6.60 ± 0.1^d	14.77 ± 0.6	19.68 ± 0.8
4e	12.95 ± 0.2	12.44 ± 0.1	18.20 ± 0.5	47.39 ± 1.8
4f	5.66 ± 0.1^d	2.89 ± 0.1^d	4.46 ± 0.1^d	9.33 ± 0.3^d
4g	12.88 ± 0.6	8.68 ± 0.1	17.38 ± 0.5	NT ^c
4h	41.81 ± 1.6	37.53 ± 0.8	48.83 ± 1.4	NT ^c
4i	40.51 ± 1.1	31.86 ± 0.8	40.11 ± 1.9	NT ^c
4j	22.85 ± 0.7	32.60 ± 0.9	43.30 ± 1.8	NT ^c
4k	11.71 ± 0.3	12.21 ± 0.4	13.91 ± 0.5	50.01 ± 0.4
5a	6.41 ± 0.1^d	3.34 ± 0.1^d	4.51 ± 0.6^d	9.52 ± 0.3^d
5b	18.40 ± 0.2	17.52 ± 0.7	21.75 ± 1.0	NT ^c
7a	NA ^b	NA ^b	NA ^b	NT ^c
7b	NA ^b	NA ^b	NA ^b	NT ^c
8a	35.53 ± 2.0	26.61 ± 0.9	32.12 ± 1.2	NT ^c
8b	18.65 ± 0.6	19.48 ± 0.7	18.18 ± 0.6	NT ^c
8c	17.24 ± 0.9	12.23 ± 0.3	19.02 ± 0.5	NT ^c
8d	48.57 ± 1.8	45.32 ± 1.2	NA ^b	NT ^c
8e	34.66 ± 1.0	27.79 ± 0.5	25.82 ± 0.6	NT ^c
8f	8.96 ± 0.2^d	3.23 ± 0.1^d	7.65 ± 0.2^d	11.59 ± 0.2
8g	6.59 ± 0.1^d	4.69 ± 0.1^d	9.29 ± 0.1^d	14.17 ± 0.3
8h	12.03 ± 0.3	10.32 ± 0.6	20.00 ± 0.4	38.37 ± 1.4
8i	15.55 ± 0.4	12.52 ± 0.2	22.69 ± 0.7	47.77 ± 2.1
8j	NA ^b	NA ^b	NA ^b	NT ^c
8k	5.55 ± 0.1^d	4.58 ± 0.1^d	9.15 ± 0.2^d	13.50 ± 0.8
8l	10.28 ± 0.1	3.73 ± 0.1^d	7.89 ± 0.5^d	13.16 ± 0.9
9a	24.18 ± 0.7	21.90 ± 0.9	33.59 ± 0.9	39.11 ± 1.0
9b	NA ^b	45.09 ± 0.7	NA ^b	NT ^c
Colchicine	9.30 ± 0.2	7.44 ± 0.2	10.45 ± 0.3	10.65 ± 0.2

^a IC₅₀ values are the mean ± S.D. of three separate experiments. ^b NA: compounds having IC₅₀ value > 50 μM. ^c NT: compounds not tested for their tubulin polymerization assay. ^d Bold figures indicate superior potency than colchicine.

signals of NH group at 8.20 ppm, and singlet signals of NH₂ at a range of 10.04–10.12 ppm.

For compounds **4a–k**, **5a,b**, **8a–l**, and **9a,b** the IR spectra showed absorption bands at ranges of 3115–3441, 1688–1722 and 1605–1648 corresponding to NH, C=O, C=N groups, respectively. The ¹H NMR spectrum of **4a–k**, **5a,b**, **8a–l**, and **9a,b** showed characteristic peaks attributed to imine methyl protons between 2.47 ppm and 3.92 ppm. The proton present in the Schiff base appeared at a range of 8.25–8.66 ppm. The characteristic peaks due to NH proton appeared between 10.07 and 12.87 ppm as singlet peaks. The ¹³C NMR spectra of compounds **4a–k**, **5a,b**, **8a–l**, and **9a,b** provided additional evidence in support of the proposed structures. All spectra that supports elucidating the chemical structures of the new derivatives are supplied with this research work as ESI file.†

2.2. Biological evaluation

2.2.1. In vitro anti-proliferative activity. The synthesized compounds were tested for their *in vitro* cytotoxic activities using standard MTT method,^{49–51} against a group of human

cancer cell lines namely; colorectal carcinoma (HCT-116), hepatocellular carcinoma (HepG-2), and breast cancer (MCF-7). Colchicine was used as a positive control. The results of cytotoxicity test were reported as growth inhibitory concentration (IC₅₀) values and summarized in Table 1.

The tested compounds exhibited different degrees of anti-proliferative activities against the three tested cell lines. Their activities range from excellent, good, moderate to weak.

In general, compounds **4f**, **5a**, **8f**, **8g**, and **8k** showed superior antiproliferative activities against the three cell lines with IC₅₀

Table 2 Effect of compound **5a** on cell cycle progression in HepG-2 cells

Sample	Cell cycle distribution (%)			
	% G0-G1	% S	% G2-M	% Pre-G1
5a/HepG-2	40.17	39.28	20.55	15.33
Cont. HepG-2	56.76	38.15	5.09	2.14



Cell Cycle Analysis

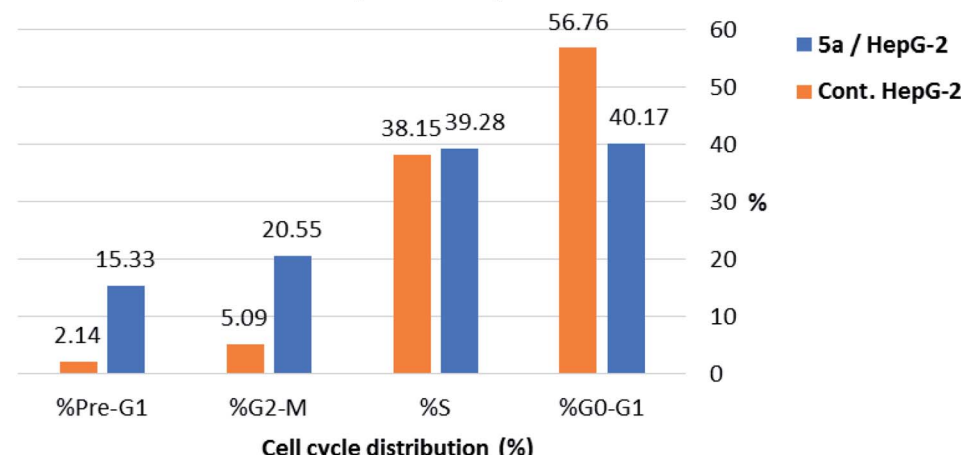


Fig. 8 Cell cycle analysis and apoptosis effect in HepG-2 cell line when treated with compound 5a.

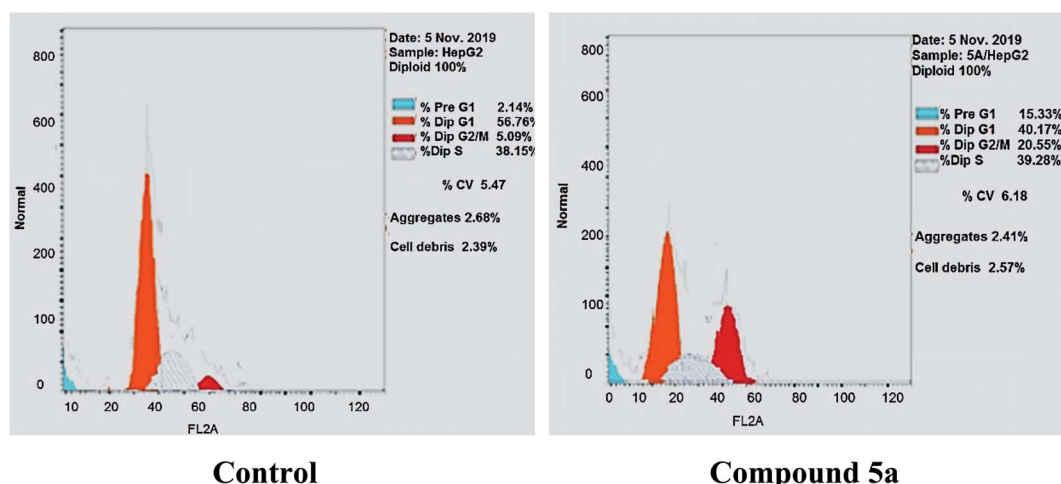


Fig. 9 HepG-2 cells distribution upon treatment with compound 5a.

values ranging from 2.89 to 9.29 μM . The cytotoxic activities of such compounds were higher than that of the reference drug, colchicine ($\text{IC}_{50} = 9.30, 7.44$, and $10.45 \mu\text{M}$ against HCT-116, HepG-2, and MCF-7, respectively). Compound **4f**, as representative example, was 1.64, 2.57 and 2.34 times as active as colchicine against HCT-116, HepG-2, and MCF-7, respectively. Also, compound **5a**, was 1.45, 2.23 and 2.32 times as active as colchicine against HCT-116, HepG-2, and MCF-7, respectively.

Additionally, compound **8l** exhibited superior activities against HepG-2, and MCF-7 with IC_{50} values of 3.73 and 7.89 μM , respectively, whereas, compound **4d** was higher than colchicine against only HepG-2 cells with IC_{50} value of $6.60 \mu\text{M}$.

Moreover, several compounds such as **4e**, **4g**, **4k**, **8b**, **8c**, and **8h** demonstrated strong anti-proliferative activities over all examined cell lines with IC_{50} values ranging from 10.32 to 20.00 μM . Also, compounds **3b**, **4b**, **4d**, **5b**, and **8i** showed strong anti-proliferative activities against only two cell lines with IC_{50} values ranging from 10.64 to 18.40 μM .

Additionally, compounds **4b**, **4j**, **5b**, **8a**, **8e**, **8i**, and **9a** displayed moderate anti-proliferative activities against at least one cell line with IC_{50} values ranging from 21.90 to 27.79 μM .

On the other hand, compounds **4a**, **4c**, **4h**, **4i**, **4j**, **8a**, and **8d** displayed weak anti-proliferative activities against at least two cell lines with IC_{50} values ranging from 31.86 to 48.83 μM .

Finally, compounds **3a**, **7a**, **7b**, and **8j** showed no activity against any of the tested cancer cell lines. In addition,

Table 3 Apoptosis and necrosis percent induced by compound 5a in HepG-2 cells

Sample	Apoptosis			
	Total	Early	Late	Necrosis
5a/HepG-2	15.33	8.25	5.54	1.54
Cont. HepG-2	2.14	1.02	0.64	0.48



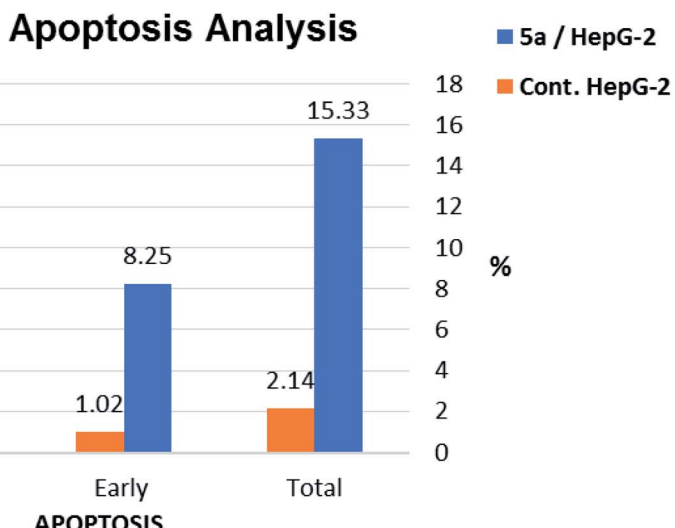


Fig. 10 Percentage of induced cell death by compound 5a on HepG-2 cells.

compound **9b** was inactive against HCT-116 and MCF-7 and compounds **4a**, **8d** revealed to be inactive against MCF-7 only.

2.2.2. Tubulin polymerization assay. To investigate whether the cytotoxic activity of the synthesized compounds was related to an interaction with the tubulin system, an *in vitro* tubulin polymerization assay was performed for the most cytotoxic members. The inhibition assay on microtubule polymerization was evaluated turbidimetrically using a fluorescent plate reader.⁵² Colchicine was used as a positive control (Table 1).

Compounds **4f** and **5a** were the most potent tubulin polymerization inhibitors with an IC_{50} values of 9.33 and 9.52 nM, respectively. These compounds had activities higher than that of colchicine ($IC_{50} = 10.65$ nM). Additionally, compounds **8f**, **8k**, and **8l** showed promising activities nearly equal to colchicine with IC_{50} values of 11.59, 13.50, and 13.16 nM, respectively. Also, compounds **4d** and **8g** showed strong tubulin

polymerization inhibitory activities with IC_{50} values of 19.68 and 14.17 nM, respectively. Finally, compounds **3b**, **4e**, **4k**, **8h**, **8i** and **9a** exhibited moderate tubulin polymerization inhibitory activities with IC_{50} values ranging from 38.37 to 50.01 nM. The results strongly implicated a direct interaction between the examined compounds and tubulin. It can be concluded that the cytotoxic activity of the synthesized compounds may derive from an interaction with tubulin and an interference with microtubule assembly.

2.2.3. Cell cycle analysis. To gain a better insight into the impact of compound **5a** on cancer cell growth inhibition, its impact on cell cycle distribution and apoptosis induction was assessed using HepG-2 cells according to the method outlined by Wang *et al.*⁵³ In fact, anticancer agents hinder cancer cell growth and multiplication by arresting cell division at distinct checkpoints, and that cells resist apoptosis are highly resistant to cancer treatment.⁵⁴ In the present work, HepG-2 cell line was

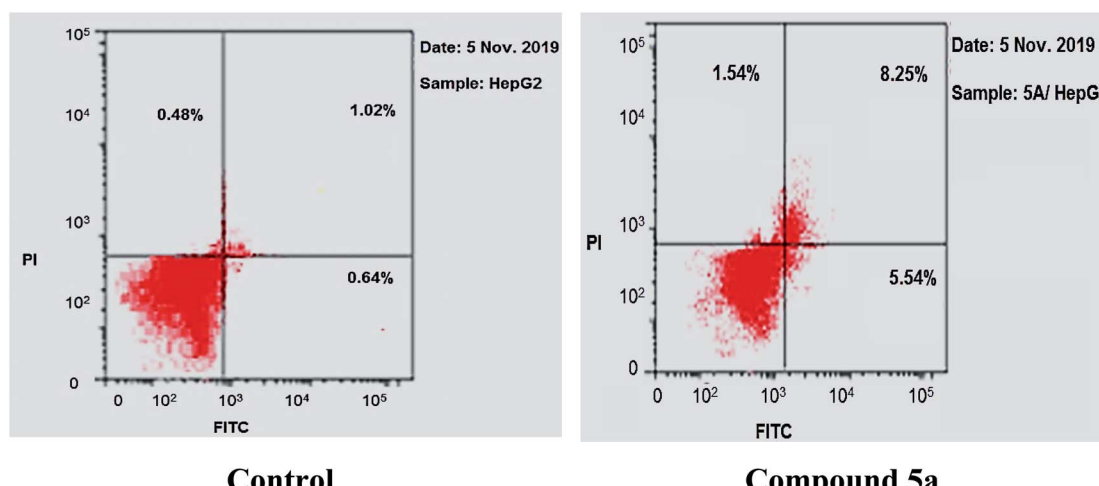


Fig. 11 Induced apoptosis on HepG-2 cells by compound 5a.



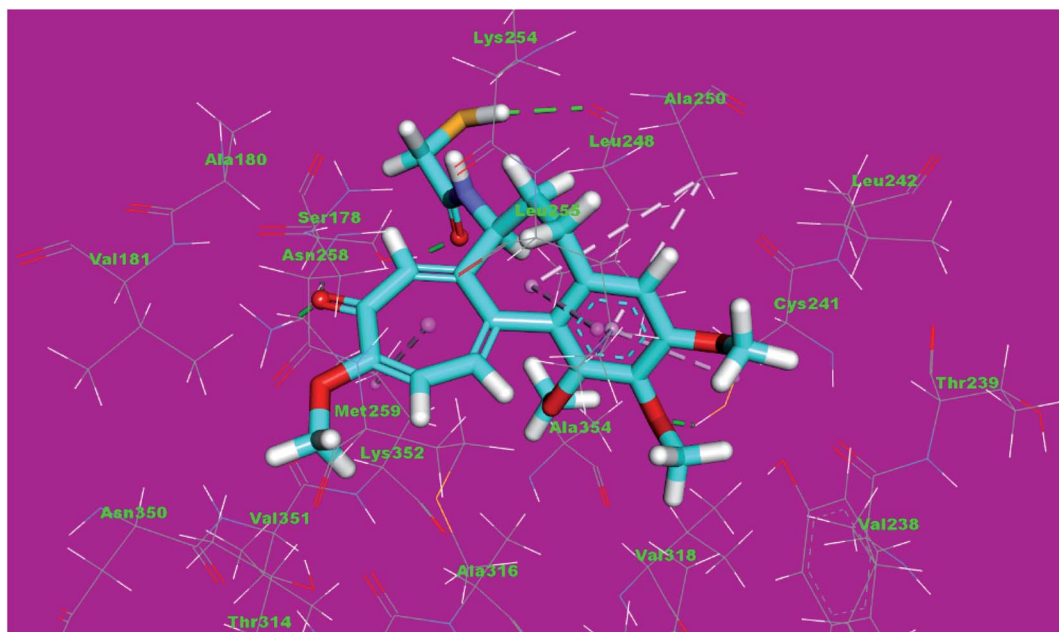


Fig. 12 3D structure of co-crystallized ligand, DAMA-colchicine, docked into the active site of tubulin.

treated with compound **5a** at a concentration equals its IC_{50} value on tubulin (9.52 nM) for 24 h.

As shown in Table 2, Fig. 8 and 9, the percentage of HepG-2 cells at S phase was increased from 38.15% to 39.28% after incubation with compound **5a**. Additionally, cells in G2/M phase markedly increased from 5.09% to 20.55% and the G1 phase decreased from 56.76% in control to 40.17%, indicating that compound **5a** caused cell arrest at G2/M phase. Also, it was found that the cells increased from 2.14% to 15.33% at pre-G1

phase, indicating that compound **5a** caused apoptosis at pre-G1 phase.

2.2.4. Annexin V-FITC apoptosis assay. To further confirm Apoptotic effect of compound **5a** in HepG-2 cells, Annexin V and PI double staining assay was performed.⁵⁵ In this test, HepG-2 cells were incubated with compound **5a** at concentration of 2.5 μ M for 24 h. The results were reported in Table 3, Fig. 10 and 11.

The results revealed that compound **5a** induced total apoptotic effect equal 13.79% which was eight time more than

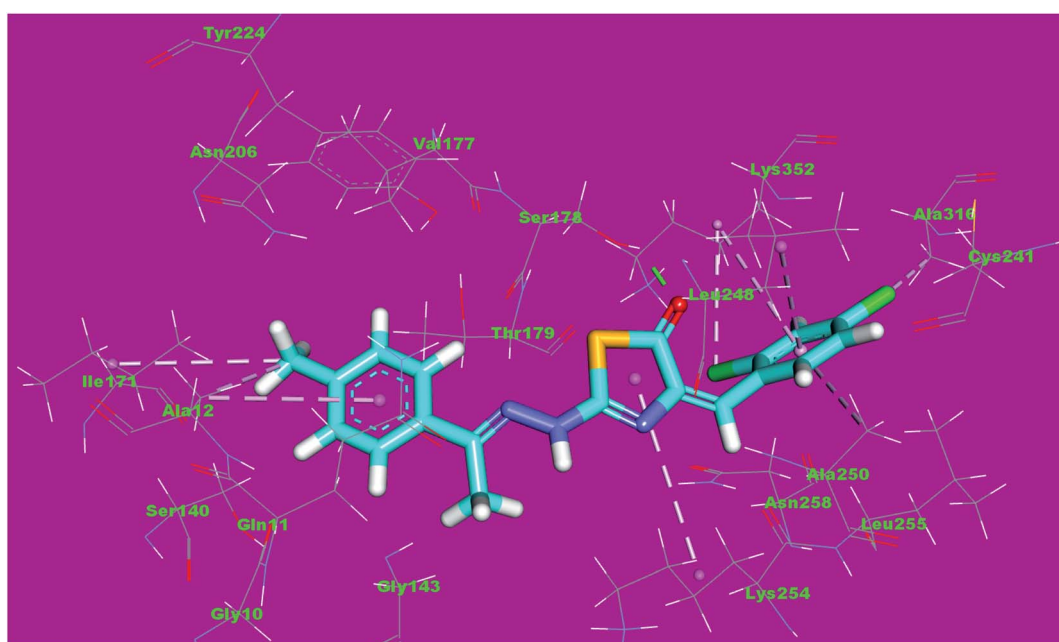


Fig. 13 3D structure of compound **4d** docked into the active site of tubulin.



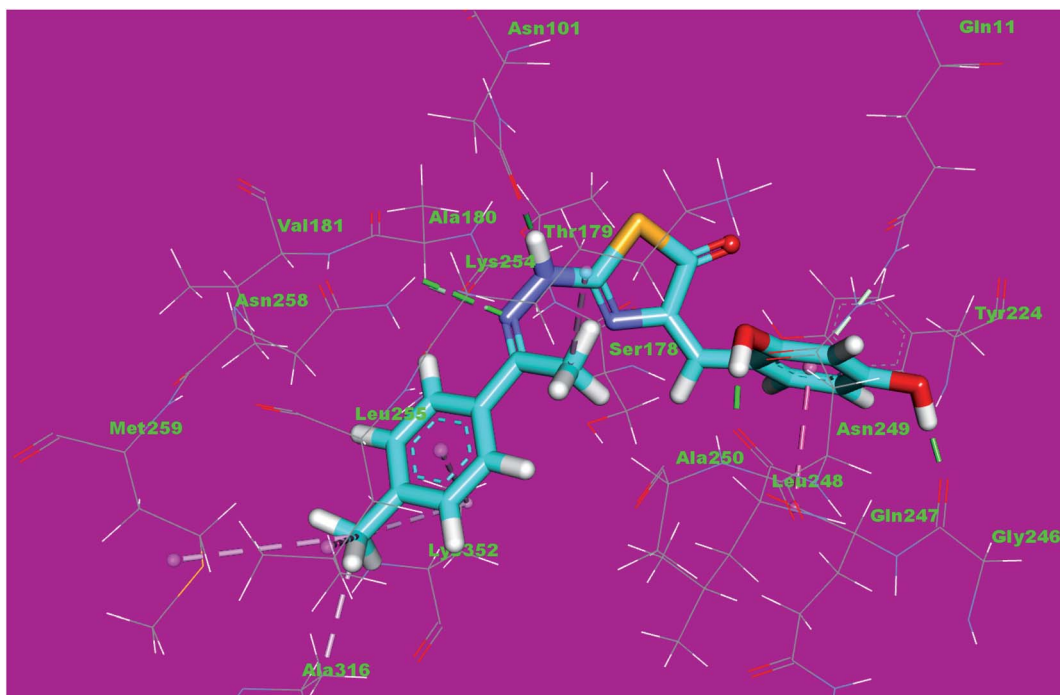


Fig. 14 3D structure of compound **4f** docked into the active site of tubulin.

the control (1.66%). In details, compound **5a** obviously induced early apoptosis by 8.25% and enhanced late apoptosis by 5.54% when compared with the untreated control HepG-2 cells (1.02% and 0.64%, respectively).

2.3. Docking studies

Molecular docking studies were conducted to give a guidance of molecular binding modes of the tested molecules inside the

pocket of tubulin heterodimers. The selected compounds have been docked against tubulin heterodimers using MOE2014 to determine the free energy and binding mode. The selection of the most promising molecules depended on the right binding mode and the binding free energy (ΔG).⁵⁶

The binding free energies of the synthesized compounds and the reference ligand were summarized in Table 4. The binding mode of the co-crystallized ligand, DAMA-colchicine, exhibited

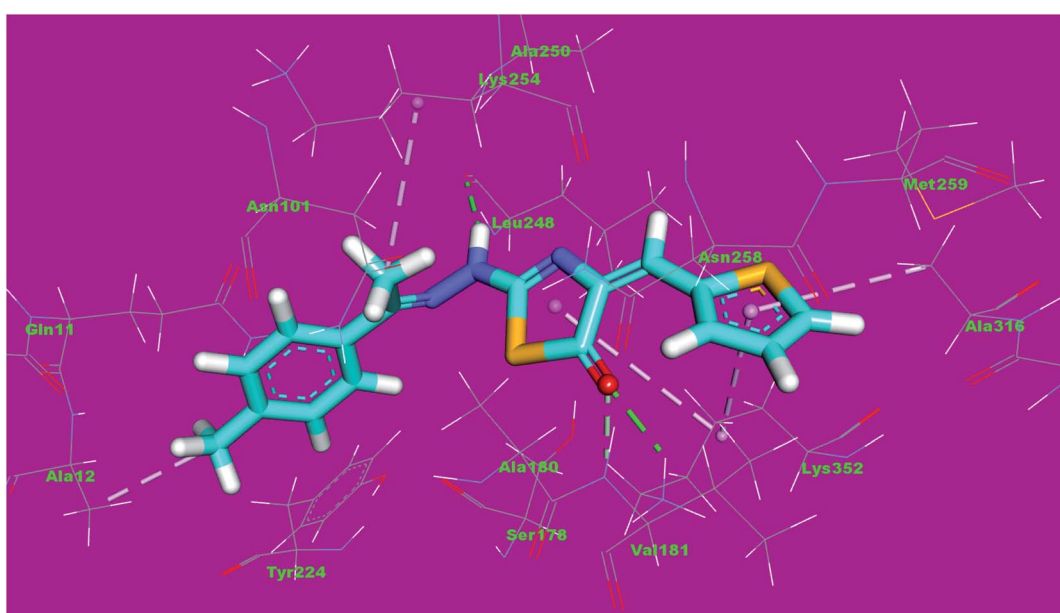


Fig. 15 3D structure of compound **5a** docked into the active site of tubulin.



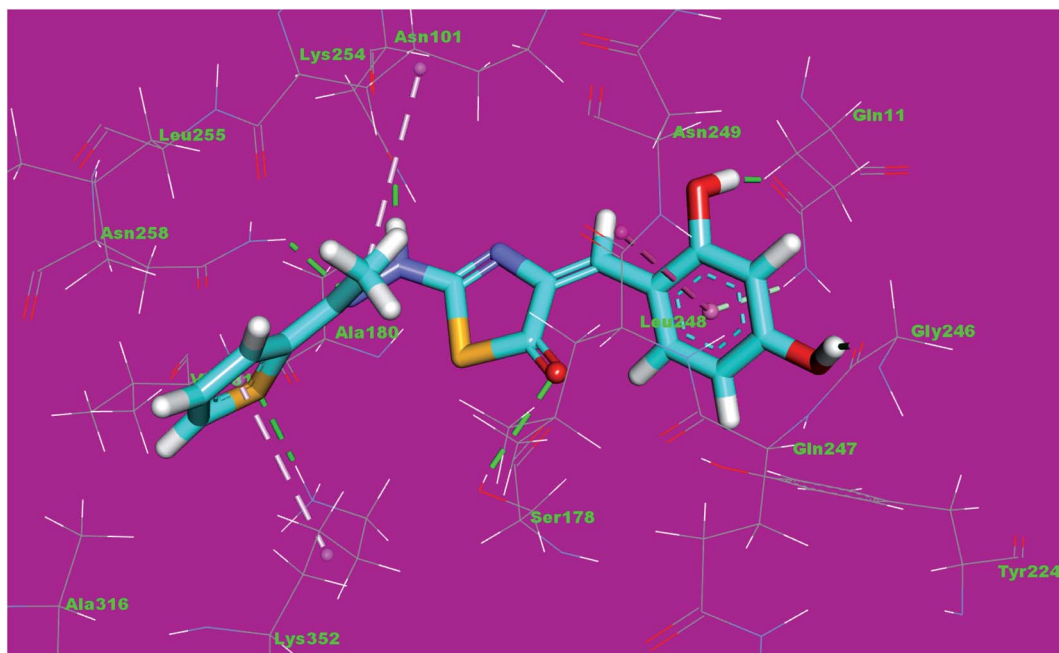


Fig. 16 3D structure of compound **8f** docked into the active site of tubulin.

an energy binding of $-13.08 \text{ kcal mol}^{-1}$. The ring A (trimethoxy phenyl moiety) formed a hydrogen bond with Cys241. Also, it formed five hydrophobic interactions with Ala250, Leu255 and Cys241. The 2-mercaptoacetamide moiety formed two hydrogen bonds with Leu248 and Ser178. The ring C formed one hydrogen bonding and one hydrophobic interaction with Lys352 (Fig. 12).

Compound **4d** as a representative example showed a binding mode like that of DAMA-colchicine, with affinity value of $-11.44 \text{ kcal mol}^{-1}$. The 2,4-dichlorophenyl moiety formed five hydrophobic interactions with Ala316, Lys352, Leu248 and Ala250. The thiazol moiety formed one hydrogen bond with Ser178 and one hydrophobic interaction with Lys254. The *p*-tolyl moiety formed three hydrophobic interactions with Ile171 and Ala12 (Fig. 13).

The binding mode of compound **4f** exhibited an affinity value of $-11.80 \text{ kcal mol}^{-1}$. The 2,4-dihydroxybenzyl moiety formed two hydrogen bonds with Gly246 and Leu248. Also, it formed two hydrophobic interactions with Gln247 and Gln11. The hydrazinyl moiety formed two hydrogen bonds with Asn258 and Asn101. The *p*-tolyl moiety formed five hydrophobic interactions with Leu255, Met259, Ala316, and Lys352 (Fig. 14).

The binding mode of compound **5a** exhibited an affinity value of $-10.41 \text{ kcal mol}^{-1}$. The thiophene moiety formed two hydrophobic interactions with Ala316 and Lys352. The hydrazinylthiazol moiety formed two hydrogen bonds with Lys352 and Lys254. Also, it formed one hydrophobic interaction with Lys352. The *p*-tolyl moiety formed one hydrophobic interaction with Ala12 (Fig. 15).

The binding mode of compound **8f** exhibited an affinity value of $-13.19 \text{ kcal mol}^{-1}$. The 2,4-dihydroxyphenyl moiety formed two hydrogen bonds with Gln11 and Gly246. In addition, it formed one hydrophobic interaction with Leu248. The

hydrazinylthiazol moiety formed three hydrogen bonds with Ser178, Asn101 and Asn258. The thiophene moiety formed one hydrophobic interaction and one hydrogen bond with Lys352 (Fig. 16).

2.4. Structure-activity relationship (SAR)

As outlined in the rationale molecular design, it was aimed at studying the SAR of the newly synthesized thiazol-5(4*H*)-one derivatives as potential tubulin polymerization inhibitors.

Initially, the effect of the ring A on the activity was explored. Comparing the cytotoxic activity of compounds **5a** incorporating thiophen-2-ylmethylene as a ring A with compounds **4f** incorporating substituted benzylidene as a ring A, indicated

Table 4 The docking binding free energies of the synthesized and co-crystallized ligand (DAMA-colchicine) compounds against tubulin

Comp.	Binding free energy (kcal mol ⁻¹)	Comp.	Binding free energy (kcal mol ⁻¹)
4a	-9.67	8b	-10.18
4b	-10.72	8c	-10.08
4c	-9.35	8d	-11.11
4d	-11.44	8e	-13.19
4e	-12.44	8f	-9.99
4f	-11.80	8g	-11.00
4g	-12.55	8h	-10.31
4h	-12.22	8i	-10.02
4i	-12.53	8j	-10.98
4j	-12.20	8k	-12.28
4k	-14.35	8L	-10.15
5a	-10.41	9a	-9.26
5b	-12.71	9b	-10.52
8a	-10.48	DAMA-colchicine	-13.08

Table 5 Reaction time and yield of both conventional, ultrasonic and microwave assisted synthesis of the synthesized compounds

Comp.	Time (min)			Yield		
	C ^a	US ^a	MW ^a	C ^a	US ^a	MW ^a
4a	180 + 240	10 + 15	2 + 2	55	77	88
4b	180 + 240	10 + 15	2 + 2	54	79	90
4c	180 + 240	10 + 15	2 + 2	56	77	88
4d	180 + 240	10 + 15	2 + 2	54	66	90
4e	180 + 240	10 + 15	2 + 2	57	60	92
4f	180 + 240	10 + 15	2 + 2	49	62	93
4g	180 + 240	10 + 15	2 + 2	58	67	92
4h	180 + 240	10 + 15	2 + 2	55	78	90
4i	180 + 240	10 + 15	2 + 2	53	62	95
4j	180 + 240	10 + 15	2 + 2	56	78	91
4k	180 + 240	10 + 15	2 + 2	50	77	88
5a	180 + 240	10 + 15	2 + 2	57	68	92
5b	180 + 240	10 + 15	2 + 2	60	77	93
8a	180 + 240	10 + 15	2 + 2	62	79	94
8b	180 + 240	10 + 15	2 + 2	56	71	93
8c	180 + 240	10 + 15	2 + 2	54	62	95
8d	180 + 240	10 + 15	2 + 2	55	78	91
8e	180 + 240	10 + 15	2 + 2	51	77	88
8f	180 + 240	10 + 15	2 + 2	52	79	90
8g	180 + 240	10 + 15	2 + 2	56	79	90
8h	180 + 240	10 + 15	2 + 2	50	70	92
8i	180 + 240	10 + 15	2 + 2	53	73	93
8j	180 + 240	10 + 15	2 + 2	55	67	90
8k	180 + 240	10 + 15	2 + 2	45	69	95
8l	180 + 240	10 + 15	2 + 2	54	78	91
9a	180 + 240	10 + 15	2 + 2	60	60	90
9b	180 + 240	10 + 15	2 + 2	61	77	94

^a C: conventional, US: ultrasonic, MW: microwave.

that the substituted benzylidene is more advantageous than thiophen-2-ylmethylene moiety. For the substituted benzylidene, the cytotoxic activities were decreased in the order of 3,4-dimethoxy benzylidene **8k** > 4-methoxy benzylidene **8g** > 2,4-dihydroxy benzylidene **8l** > 4-chloro benzylidene **8h** > 4-hydroxy benzylidene **8i** > 2,4-dichloro benzylidene **8j**.

Then, the impact of the ring C was investigated. The decreased IC₅₀ values of compounds **4c**, **4d**, **4e**, and **4f** incorporated 1-ethyl-4-methylbenzene as ring C, than those of their corresponding members **4h**, **4i**, **4j**, and **4k** incorporating 1-ethyl-4-methoxybenzene as ring C, indicated that 1-ethyl-4-methylbenzene moiety is advantageous. Also, the decreased IC₅₀ value of compound **5a** incorporating 1-ethyl-4-methylbenzene as ring C than the corresponding member **5b** 1-ethyl-4-methoxybenzene as ring C, confirm the positive effect of 1-ethyl-4-methylbenzene moiety. In addition, the higher activity of compound **9a** incorporated 2-ethylthiophene moiety as ring C than compounds **9b** with 2-ethylfuran moiety, revealed that 2-ethylthiophene moiety is more preferred biologically than 2-ethylfuran one.

3. Conclusion

To sum up, thirty-one new derivatives based on thiazol-5(4H)-one were designed and eco-friendly synthesized using

conventional, ultrasound irradiation and microwave-assisted methods. The synthesized derivatives were evaluated for their anti-proliferative activities against a group of three human cancer cell lines including; colorectal carcinoma (HCT-116), hepatocellular carcinoma (HepG-2), and breast cancer (MCF-7) using MTT assay. Compound **4f** has appeared as the most active member against all examined cells with IC₅₀ values of 5.66 ± 0.1, 2.89 ± 0.1, and 4.46 ± 0.1 μM, respectively, as it was 1.64, 2.57 and 2.34 times more active than colchicine (IC₅₀ = 9.30 ± 0.2, 7.44 ± 0.2, and 10.45 ± 0.3 μM, respectively). In addition, compounds **5a**, **8f**, **8g** and **8k** showed excellent anti-proliferative activity against the three tested cell lines with IC₅₀ values ranging from 3.23 to 9.29 μM. Moreover, the most active compounds have been studied for their inhibitory activities of tubulin polymerization. Tubulin polymerization assay findings were consistent with cytotoxicity data results. Moreover, compound **5a** arrested the cell cycle in the G2/M phase and induced apoptosis in HepG-2 cells. Docking experiments assisted these findings by anticipating potential binding interactions between the target compounds and the active sites of tubulin heterodimers. The most effective candidates in the quest for strong and selective antineoplastic agents will serve as valuable lead compounds and merit further investigations.

4. Experimental

4.1. Chemistry

All melting points were measured on a Gallen Kamp melting point apparatus (Sanyo Gallen Kamp, UK) and were uncorrected. The Microwave reactions were done by Microsynth instrument type MA143 (Micro wave flux). The ultrasound-assisted reactions were performed in Digital Ultrasonic Cleaner CD-4830 (35 KHz, 310 W). The IR spectra were recorded on a Pye-Unicam SP-3-300 infrared spectrophotometer (KBr discs) and expressed in wave number (cm⁻¹). ¹H NMR spectra were run at 300 and 400 MHz, on a Varian Mercury VX-300 and Bruker Avance III NMR spectrometer, respectively, while ¹³C NMR spectra were run at 100 MHz. TMS was used as an internal standard in deuterated dimethylsulphoxide (DMSO-*d*₆). The mass spectra were recorded on Shimadzu GCMS-QP-1000EX mass spectrometer at 70 eV. Elemental analyses were performed on CHN analyzer and all compounds were within ± 0.4 of the theoretical values. The reactions were monitored by thin-layer chromatography (TLC) using TLC sheets coated with UV fluorescent silica gel Merck 60 F254 plates and were visualized using UV lamp and different solvents as mobile phases. All reagents and solvents were purified and dried by standard techniques.

4.1.1. General procedure for synthesis of compounds **3a,b & **7a,b**.** A solution of thiosemicarbazide (10 mmol) and aryl ketones (10 mmol) namely, 4-methyl acetophenone **1a**, 3,4-methoxy acetophenone **1b**, 2-acetyl thiophene **6a** and 2-acetyl furan **6b**, in anhydrous ethanol (20 mL) and few drops of g. acetic acid was refluxed for 2 h. The formed product was filtered, washed with ethanol, dried and crystallized from ethanol to give compounds **3a,b** & **7a,b**, respectively.



4.1.1.1. (*E*)-2-(1-(*p*-Tolyl)ethylidene)hydrazine-1-carbothioamide (3a**).** White crystals; mp 240–242 °C; IR (KBr, cm^{-1}): 3376, 3230, 3151 (NH₂, NH), 3053 (CH aromatic), 2933 (CH aliphatic), 1590 (C=N); ¹H NMR (DMSO-*d*₆) δ ppm: 2.32 (s, 3H, CH₃), 2.41 (s, 3H, CH₃), 7.16 (d, 2H, *J* = 6.6 Hz, Ar–H, H₃, H₅ of phenyl), 7.44 (d, 2H, *J* = 6.6 Hz, Ar–H, H₂, H₆ of phenyl), 8.20 (s, 2H, NH₂, D₂O exchangeable), 10.12 (s, 1H, NH, D₂O exchangeable); anal. calcd for C₁₀H₁₃N₃S (207.3): C, 57.94; H, 6.32; N, 20.27; found: C, 57.73; H, 6.22; N, 20.15%.

4.1.1.2. (*E*)-2-(1-(3,4-Dimethoxyphenyl)ethylidene)hydrazine-1-carbothioamide (3b**).** White crystals (yield 85%); mp 205–207 °C °C; IR (KBr, cm^{-1}): 3375, 3267, 3157 (NH₂, NH), 3099 (CH aromatic), 2931 (CH aliphatic), 1599 (C=N), 1245 (C=S); ¹H NMR (DMSO-*d*₆) δ ppm: 2.32 (s, 3H, CH₃), 3.80 (s, 3H, OCH₃), 6.91 (s, 3H, OCH₃), 6.97 (d, 1H, *J* = 8 Hz, Ar–H, H₅ of phenyl), 7.47 (d, 2H, *J* = 8 Hz, Ar–H, H₂, H₆ of phenyl), 8.20 (s, 2H, NH₂, D₂O exchangeable), 10.04 (s, 1H, NH, D₂O exchangeable); ¹³C NMR (DMSO-*d*₆) δ ppm: 179.0, 150.6, 149.0, 148.7, 130.8, 120.4, 111.4, 110.0, 56.1, 55.9, 14.4; anal. calcd for C₁₁H₁₅N₃O₂S (253.3): C, 52.16; H, 5.97; N, 16.59; found: C, 51.91; H, 5.88; N, 16.48%.

4.1.1.3. (*E*)-2-(1-(Thiophen-2-yl)ethylidene)hydrazine-1-carbothioamide (7a**).** White crystals (yield 75%); mp 122–124 °C; IR (KBr, cm^{-1}): 3407, 3241, 3145 (NH₂, NH), 2979 (CH aliphatic), 1606 (C=N); ¹H NMR (DMSO-*d*₆) δ ppm: 2.29 (s, 3H, CH₃), 6.47 (s, 2H, NH₂, D₂O exchangeable), 7.02–704 (m, 1H, Ar–H), 7.31 (d, 1H, Ar–H), 7.35 (d, 1H, Ar–H), 8.73 (s, 1H, NH, D₂O exchangeable); anal. calcd for C₇H₉N₃S₂ (199.0): C, 42.19; H, 4.55; N, 21.09; found: C, 41.95; H, 4.46; N, 21.00%.

4.1.1.4. (*E*)-2-(1-(Furan-2-yl)ethylidene)hydrazine-1-carbothioamide (7b**).** White crystals; mp 122–124 °C; IR (KBr, cm^{-1}): 3346, 3249, 3132 (NH₂, NH), 3053 (CH aromatic), 2933 (CH aliphatic), 1602 (C=N); ¹H NMR (DMSO-*d*₆) δ ppm: 2.26 (s, 3H, CH₃), 6.56–6.57 (m, 1H, Ar–H), 7.07 (d, 1H, Ar–H), 7.73 (s, 2H, NH₂, D₂O exchangeable), 8.25 (d, 1H, Ar–H), 10.35 (s, 1H, NH, D₂O exchangeable); anal. calcd for C₇H₉N₃OS (183.2): C, 45.89; H, 4.95; N, 22.93; found: C, 45.76; H, 4.86; N, 22.80%.

4.1.2. General procedure for synthesis of compounds **4a–k**, **5a,b**, **8a–l** & **9a,b**

4.1.2.1. Conventional method. A mixture of starting compounds **3a,b** & **7a,b** (10 mmol), chloroacetic acid (1 mmol), and the appropriate aromatic aldehyde (10 mmol) namely, 4-methoxy benzaldehyde, 4-chloro benzaldehyde, 4-hydroxy benzaldehyde, 2,4-dichloro benzaldehyde, 3,4-dimethoxy benzaldehyde, and 2,4-dihydroxy benzaldehyde was refluxed in a mixture of ethanol (20 mL) and acetic acid glacial (5 mL) for 3 h. After cooling, the formed precipitate were filtered and crystallized from methanol to afford the corresponding compounds **4a–k**, **5a,b**, **8a–l** & **9a,b**, respectively.

4.1.2.2. Under microwave method. A mixture of thiosemicarbazide (10 mmol), appropriate aryl ketones (10 mmol) namely, 4-methyl acetophenone **1a**, 3,4-methoxy acetophenone **1b**, 2-acetyl thiophene **6a** and 2-acetyl furan **6b**, and glacial acetic acid (2 mL) was added to the reaction vessel placed into the microwave reactor. The mixture was allowed to react under

microwave irradiation of 200–400 W at 120 °C for 2 min. After the reaction completion (monitored by TLC), a mixture of chloroacetic acid (10 mmol) and appropriate aromatic aldehydes (10 mmol) namely, 4-methoxy benzaldehyde, 4-chloro benzaldehyde, 4-hydroxy benzaldehyde, 2,4-dichloro benzaldehyde, 3,4-dimethoxy benzaldehyde, and 2,4-dihydroxy benzaldehyde was added to the reaction vessel. The reaction mixture was then subjected to microwave irradiation of 200–400 W at 120 °C for 2 min. with continuous stirring *via* the automatic mode. The reaction was monitored using TLC. After completion of the reaction and cooling, the product was obtained and crystallized from the proper solvent to give the corresponding title compounds **4a–k**, **5a,b**, **8a–l** & **9a,b**.

4.1.2.3. Under sonication method. A mixture of thiosemicarbazide (10 mmol) and appropriate aryl ketones (10 mmol) namely, 4-methyl acetophenone **1a**, 3,4-methoxy acetophenone **1b**, 2-acetyl thiophene **6a** and 2-acetyl furan **6b**, in anhydrous ethanol (20 mL) with catalytic amount of glacial acetic acid was placed in Erlenmyer flask (50 mL) and subjected to ultrasound waves at room temperature for 10 min. A mixture of chloroacetic acid (10 mmol) and (1 mmol) of appropriate aromatic aldehydes namely, 4-methoxy benzaldehyde, 4-chloro benzaldehyde, 4-hydroxy benzaldehyde, 2,4-dichloro benzaldehyde, 3,4-dimethoxy benzaldehyde, and 2,4-dihydroxy benzaldehyde was added to the reaction vessel, and subjected to ultrasound waves at room temperature for 15 min. The formed precipitate was filtered, dried, and crystallized from the appropriate solvent to afford the target compounds **4a–k**, **5a,b**, **8a–l** & **9a,b**. Reaction time and yield of the conventional, ultrasonic and microwave procedures were summarized in Table 5.

4.1.2.4. 4-((*E*)-4-Methoxybenzylidene)-2-(2-((*E*)-1-(*p*-tolyl)ethylidene)hydrazinyl) thiazol-5(4H)-one (4a**).** Yellow crystals; mp 248–250 °C; IR (KBr, cm^{-1}): 3112 (NH), 3009 (CH-aromatic), 2973 (CH aliphatic), 1722 (C=O), 1636 (C=N); ¹H NMR (DMSO-*d*₆) δ ppm: 3.31 (s, 6H, 2CH₃), 3.86 (s, 3H, OCH₃), 6.98–7.06 (m, 4H, Ar–H), 7.67–7.72 (d, 4H, Ar–H), 8.31 (s, 1H, C=CH olefinic), 11.88 (s, 1H, NH, D₂O exchangeable); anal. calcd for C₂₀H₁₉N₃O₂S (365.5): C, 65.73; H, 5.24; N, 11.50; found: C, 65.51; H, 5.16; N, 11.41%.

4.1.2.5. 4-((*E*)-4-Chlorobenzylidene)-2-(2-((*E*)-1-(*p*-tolyl)ethylidene)hydrazinyl) thiazol-5(4H)-one (4b**).** Pale yellow crystals; mp 266–268 °C; IR (KBr, cm^{-1}): 3112 (NH), 3027 (CH-aromatic), 2938 (CH aliphatic), 1709 (C=O), 1644 (C=N); ¹H NMR (DMSO-*d*₆) δ ppm: 3.31 (s, 3H, CH₃), 3.88 (s, 3H, CH₃), 7.47–7.96 (m, 4H, Ar–H), 7.70–7.80 (m, 4H, Ar–H), 8.39 (s, 1H, C=CH olefinic), 11.98 (s, 1H, NH, D₂O exchangeable); anal. calcd for C₁₉H₁₆ClN₃OS (369.9): C, 61.70; H, 4.36; N, 11.36; found: C, 61.55; H, 4.26; N, 11.24%.

4.1.2.6. 4-((*E*)-4-Hydroxybenzylidene)-2-(2-((*E*)-1-(*p*-tolyl)ethylidene)hydrazinyl) thiazol-5(4H)-one (4c**).** Yellow crystals; mp 272–274 °C; IR (KBr, cm^{-1}): 3420 (OH), 3170 (NH), 3035 (CH-aromatic), 2924 (CH aliphatic), 3170 (NH), 1689 (C=O), 1638 (C=N); ¹H NMR (DMSO-*d*₆) δ ppm: 2.49 (s, 3H, CH₃), 3.85 (s, 3H, CH₃), 6.82–6.86 (m, 4H, Ar–H), 7.56–7.63 (m, 4H, Ar–H), 8.25 (s, 1H, C=CH olefinic), 9.94 (s, 1H, NH, D₂O exchangeable); anal. calcd for C₂₀H₁₉ON₃S (365.5): C, 65.73; H, 5.24; N, 11.50; found: C, 65.51; H, 5.16; N, 11.41%.



exchangeable), 11.83 (s, 1H, OH, D₂O exchangeable); anal. calcd for C₁₉H₁₇N₃O₂S (351.4): C, 64.94; H, 4.88; N, 11.96; found: C, 64.75; H, 4.80; N, 11.85%.

4.1.2.c.4. *4-((E)-2,4-Dichlorobenzylidene)-2-(2-((E)-1-(*p*-tolyl)ethylidene)hydrazinyl) thiazol-5(4H)-one (4d).* White crystals; mp > 300 °C; IR (KBr, cm⁻¹): 3115 (NH), 3066 (CH-aromatic), 2945 (CH aliphatic), 1720 (C=O), 1644 (C=N); ¹H NMR (DMSO-*d*₆) δ ppm: 3.30 (s, 3H, CH₃), 3.98 (s, 3H, CH₃), 7.47 (d, 2H, Ar-H), 7.74 (d, 2H, Ar-H), 7.94 (d, 2H, Ar-H, *J* = 8.4), 8.65 (s, 1H, C=CH olefinic), 8.66 (s, 1H of Ar-H), 12.09 (s, 1H, NH, D₂O exchangeable); anal. calcd for C₁₉H₁₅Cl₂N₃OS (404.3): C, 56.44; H, 3.74; N, 10.39; found: C, 56.28; H, 3.65; N, 10.27%.

4.1.2.c.5. *4-((E)-3,4-Dimethoxybenzylidene)-2-(2-((E)-1-(*p*-tolyl)ethylidene)hydrazinyl) thiazol-5(4H)-one (4e).* Off white crystals; mp 254–256 °C; IR (KBr, cm⁻¹): 3114 (NH), 2949 (CH aliphatic), 1704 (C=O), 1648 (C=N); ¹H NMR (DMSO-*d*₆) δ ppm: 3.32 (s, 3H, CH₃), 3.67 (s, 3H, CH₃), 3.83 (s, 3H, OCH₃), 3.88 (s, 3H, OCH₃), 6.94–7.33 (m, 6H, Ar-H), 8.27 (s, 1H, C=CH olefinic + s, 1H of Ar-H), 11.80 (s, 2H, NH, D₂O exchangeable), ¹³C NMR (DMSO-*d*₆) δ ppm: 178.2, 161.7, 160.4, 158.3, 158.1, 157.1, 153.5, 142.6, 142.0, 139.4, 130.1, 129.2 (2), 1284 (2), 112.3, 110.2, 56.6, 56.1, 33.4, 13.7; anal. calcd for C₂₁H₂₁N₃O₃S (395.5): C, 63.78; H, 5.35; N, 10.63; found: C, 63.59; H, 5.27; N, 10.50%.

4.1.2.c.6. *4-((E)-2,4-Dihydroxybenzylidene)-2-(2-((E)-1-(*p*-tolyl)ethylidene)hydrazinyl) thiazol-5(4H)-one (4f).* Red crystals; mp over 300 °C; IR (KBr, cm⁻¹): 3441 (OH), 3204 (NH), 3037 (CH-aromatic), 2935 (CH aliphatic), 1697 (C=O), 1625 (C=N); ¹H NMR (DMSO-*d*₆) δ ppm: 2.47 (s, 3H, CH₃), 3.93 (s, 3H, CH₃), 6.29–6.37 (m, 4H, Ar-H), 7.33 (d, 2H, Ar-H, *J* = 8.4), 8.47 (s, 1H, C=CH olefinic + s, 1H of Ar-H), 10.08 (s, 1H, NH, for thiazole tautomer, D₂O exchangeable), 11.02 (s, 1H, 2OH, D₂O exchangeable), 11.94 (s, 1H, NH, for thiazole tautomer D₂O exchangeable); ¹³C NMR (DMSO-*d*₆) δ ppm: 174.0, 161.8 (2), 160.6, 158.7(2), 133.0, 132.1, 110.8, 110.0, 109.0(2), 108.4(2), 102.8 (2), 102.0, 40.5, 19.7; anal. calcd for C₁₉H₁₇N₃O₃S (367.4): C, 62.11; H, 4.66; N, 11.44; found: C, 61.89; H, 4.57; N, 11.31%.

4.1.2.c.7. *2-(2-((E)-1-(3,4-Dimethoxyphenyl)ethylidene)hydrazinyl)-4-((E)-4-methoxy benzylidene) thiazol-5(4H)-one (4g).* White crystals; mp 240–242 °C; IR (KBr, cm⁻¹): 3149 (NH), 3035 (CH-aromatic), 2964 (CH aliphatic), 1721 (C=O), 1621 (C=N); ¹H NMR (DMSO-*d*₆) δ ppm: 3.82 (s, 3H, CH₃), 3.84 (s, 3H, OCH₃), 3.85 (s, 3H, OCH₃), 3.86 (s, 3H, OCH₃), 6.96 (d, 2H, Ar-H, *J* = 8 Hz), 7.01 (s, 1H, Ar-H), 7.33 (d, 2H, Ar-H, *J* = 8 Hz), 7.47 (d, 1H, Ar-H, *J* = 8 Hz), 7.68 (d, 1H, Ar-H, *J* = 8 Hz), 8.31 (s, 1H, C=CH olefinic), 11.87 (s, 1H, NH, D₂O exchangeable); ¹³C NMR (DMSO-*d*₆) δ ppm: 160.1, 152.3, 151.0, 148.8, 130.8(2), 129.7, 123.5, 120.3(2), 114.7, 111.5(2), 111.2, 110.6, 109.6 (2), 55.9, 55.7, 55.6, 14.2; anal. calcd for C₂₁H₂₁N₃O₄S (411.5): C, 61.30; H, 5.14; N, 10.21; found: C, 61.08; H, 5.04; N, 10.11%.

4.1.2.c.8. *2-(2-((E)-1-(3,4-Dimethoxyphenyl)ethylidene)hydrazinyl)-4-((E)-4-hydroxy benzylidene)thiazol-5(4H)-one (4h).* Yellow crystals; mp 290–292 °C; IR (KBr, cm⁻¹): 3231 (NH), 2924 (CH aliphatic), 1687 (CO), 1639 (C=N); ¹H NMR (DMSO-*d*₆) δ ppm:

3.43 (s, 3H, CH₃), 3.82 (s, 3H, CH₃), 3.84 (s, 3H, CH₃), 6.81 (d, 2H, Ar-H, *J* = 8.4 Hz), 6.97 (d, 2H, Ar-H, *J* = 8.4 Hz), 7.35–7.57 (m, 3H, Ar-H), 8.25 (s, 1H, C=CH olefinic), 9.96 (s, 1H, NH, D₂O exchangeable), 11.87 (s, 1H, OH, D₂O exchangeable); anal. calcd for C₂₀H₁₉N₃O₄S (397.4): C, 60.44; H, 4.82; N, 10.57; found: C, 60.24; H, 4.73; N, 10.46%.

4.1.2.c.9. *4-((E)-2,4-Dichlorobenzylidene)-2-(2-((E)-1-(3,4-dimethoxyphenyl)ethylidene)hydrazinyl) thiazol-5(4H)-one (4i).* Off white crystals; mp > 300 °C; IR (KBr, cm⁻¹): 3114, (NH), 3066 (CH-aromatic), 2944 (CH aliphatic), 1721 (CO), 1644 (C=N); ¹H NMR (DMSO-*d*₆) δ ppm: 3.78 (s, 3H, CH₃), 3.82 (s, 3H, OCH₃), 3.91 (s, 3H, OCH₃), 7.51–7.62 (m, 3H, Ar-H), 7.94 (m, 2H, Ar-H, *J* = 8.4 Hz), 8.56 (s, 1H, C=CH olefinic + 1H, Ar-H), 12.06 (s, 1H, NH, D₂O exchangeable); anal. calcd for C₂₀H₁₇C₁₂N₃O₃S (450.3): C, 53.34; H, 3.81; N, 9.33; found: C, 53.15; H, 3.72; N, 9.22%.

4.1.2.c.10. *4-((E)-3,4-Dimethoxybenzylidene)-2-(2-((E)-1-(3,4-dimethoxyphenyl)ethylidene)hydrazinyl)thiazol-5(4H)-one (4j).* Yellow crystals; mp 232–236 °C; IR (KBr, cm⁻¹): 3433, (NH), 2944 (CH aliphatic), 1707 (CO), 1648 (C=N); ¹H NMR (DMSO-*d*₆) δ ppm: 3.61 (s, 3H, CH₃), 3.74 (s, 3H, OCH₃), 3.79 (s, 3H, OCH₃), 3.81 (s, 3H, OCH₃), 3.86 (s, 3H, OCH₃), 6.99 (d, 1H, Ar-H, *J* = 8 Hz), 7.05–7.15 (m, 3H, Ar-H), 7.55 (s, 1H, Ar-H), 8.29 (s, 1H, C=CH olefinic + 1H, Ar-H), 11.91 (s, 1H, NH, D₂O exchangeable); anal. calcd for C₂₂H₂₃N₃O₅S (441.5): C, 59.85; H, 5.25; N, 9.52; found: C, 59.66; H, 5.17; N, 9.60%.

4.1.2.c.11. *4-((E)-2,4-Dihydroxybenzylidene)-2-(2-((E)-1-(3,4-dimethoxyphenyl)ethylidene)hydrazinyl)thiazol-5(4H)-one (4k).* Red crystals; mp > 300 °C; IR (KBr, cm⁻¹): 3214, (NH), 3053 (CH-aromatic), 2975 (CH aliphatic), 1697 (CO), 1633 (C=N); ¹H NMR (DMSO-*d*₆) δ ppm: 3.38 (s, 3H, CH₃), 3.77 (s, 3H, OCH₃), 3.86 (s, 3H, OCH₃), 6.29–6.38 (m, 3H, Ar-H), 7.31 (d, 2H, Ar-H), 8.47 (s, 1H, C=CH olefinic + 1H, Ar-H), 10.08 (s, 1H, NH, for thiazol tautomer, D₂O exchangeable), 11.02 (s, 2H, OH, D₂O exchangeable), 11.95 (s, 1H, NH, for thiazole tautomer, D₂O exchangeable); anal. calcd for C₂₀H₁₉N₃O₅S (413.4): C, 58.10; H, 4.63; N, 10.16; found: C, 57.26; H, 4.55; N, 10.06%.

4.1.2.c.12. *(E)-4-(Thiophen-2-ylmethylene)-2-(2-((E)-1-(*p*-tolyl)ethylidene)hydrazinyl) thiazol-5(4H)-one (5a).* Orange crystals; mp 202–204 °C; IR (KBr, cm⁻¹): 3122 (NH), 3051 (CH-aromatic), 2950 (CH aliphatic), 1707 (C=O), 1634 (C=N); ¹H NMR (DMSO-*d*₆) δ ppm: 3.86 (s, 6H, 2CH₃), 7.06 (d, 2H, Ar-H, *J* = 8), 7.14 (m, 1H, Ar-H), 7.26 (d, 2H, Ar-H, *J* = 8), 7.56 (d, 1H, Ar-H), 7.73 (m, 1H, Ar-H), 8.66 (s, 1H, C=CH olefinic), 11.75 (s, 1H, NH, D₂O exchangeable); anal. calcd for C₁₇H₁₅N₃OS₂ (341.4): C, 59.80; H, 4.43; N, 12.31; found: C, 59.69; H, 4.35; N, 12.19%.

4.1.2.c.13. *(E)-2-(2-((E)-1-(3,4-Dimethoxyphenyl)ethylidene)hydrazinyl)-4-(thiophen-2-ylmethylene)thiazol-5(4H)-one (5b).* Pale yellow crystals; mp 208–210 °C; IR (KBr, cm⁻¹): 3411, (NH), 3053 (CH-aromatic), 2951 (CH aliphatic), 1709 (CO), 1633 (C=N); ¹H NMR (DMSO-*d*₆) δ ppm: 3.79 (s, 3H, CH₃), 3.82 (s, 3H, OCH₃), 3.85 (s, 3H, OCH₃), 7.13–7.18 (m, 2H, Ar-H), 7.47–7.48 (d, 1H, Ar-H), 7.67 (d, 2H, Ar-H, *J* = 5.2 Hz), 8.52 (s, 1H, C=CH olefinic + 1H, Ar-H), 11.90 (s, 1H, NH, D₂O exchangeable); anal. calcd for



$\text{C}_{18}\text{H}_{17}\text{N}_3\text{O}_3\text{S}_2$ (387.5): C, 55.80; H, 4.42; N, 10.84; found: C, 55.69; H, 4.33; N, 10.72%.

4.1.2.c.14. *4-((E)-4-Methoxybenzylidene)-2-(2-((E)-1-(thiophen-2-yl)ethylidene)hydra-zinyl)thiazol-5(4H)-one (8a).* White crystals; mp 243–245 °C; IR (KBr, cm^{-1}): 3287, 3149, (NH), 3075 (CH-aromatic), 2934 (CH aliphatic), 1709 (C=O), 1605 (C=N); ^1H NMR (DMSO- d_6) δ ppm: 3.77 (s, 3H, CH_3), 3.85 (s, 3H, OCH_3), 6.98–7.02 (m, 3H, Ar-H), 7.66–7.69 (m, 4H, Ar-H), 8.31 (s, 1H, C=CH olefinic), 11.74 (s, 1H, NH, D_2O exchangeable); anal. calcd for $\text{C}_{17}\text{H}_{15}\text{N}_3\text{O}_2\text{S}_2$ (357.4): C, 57.12; H, 4.23; N, 11.76; found: C, 56.90; H, 4.16; N, 11.64%.

4.1.2.c.15. *4-((E)-4-Chlorobenzylidene)-2-(2-((E)-1-(thiophen-2-yl)ethylidene)hydra-zinyl)thiazol-5(4H)-one (8b).* Orange crystals; mp 252–254 °C; IR (KBr, cm^{-1}): 3145 (NH), 3043 (CH-aromatic), 2936 (CH aliphatic), 1714 (C=O), 1640 (C=N); ^1H NMR (DMSO- d_6) δ ppm: 3.93 (s, 3H, CH_3), 7.56–7.70 (m, 3H, Ar-H), 7.83–8.28 (m, 3H, Ar-H), 8.94 (s, 1H, C=CH olefinic H), 9.02 (dd, 1H, Ar-H), 12.03 (s, 1H, NH, D_2O exchangeable); ^{13}C NMR (DMSO- d_6) δ ppm: 163.2, 153.2, 139.2, 138.3, 138.1, 137.4, 137.2, 136.4, 135.3, 130.1(2), 129.1(2), 121.2, 120.9, 14.1; anal. calcd for $\text{C}_{16}\text{H}_{12}\text{ClN}_3\text{OS}_2$ (361.9): C, 53.11; H, 3.34; N, 11.61; found: C, 52.99; H, 3.26; N, 11.50%.

4.1.2.c.16. *4-((E)-4-Hydroxybenzylidene)-2-(2-((E)-1-(thiophen-2-yl)ethylidene)hydra-zinyl)thiazol-5(4H)-one (8c).* Orange crystals; mp 178–180 °C; IR (KBr, cm^{-1}): 3235 (OH), 3181 (NH), 3035 (CH-aromatic), 2964 (CH aliphatic), 1688 (C=O), 1641 (C=N); ^1H NMR (DMSO- d_6) δ ppm: 3.84 (s, 3H, CH_3), 6.80–6.82 (m, 4H, Ar-H), 7.55–7.57 (m, 3H, Ar-H), 8.24 (s, 1H, C=CH olefinic), 9.96 (s, 1H, NH, D_2O exchangeable), 11.82 (s, 1H, OH, D_2O exchangeable); anal. calcd for $\text{C}_{16}\text{H}_{13}\text{N}_3\text{O}_2\text{S}_2$ (343.4): C, 55.96; H, 3.82; N, 12.24; found: C, 55.79; H, 3.75; N, 12.11%.

4.1.2.c.17. *4-((E)-2,4-Dichlorobenzylidene)-2-(2-((E)-1-(thiophen-2-yl)ethylidene)hydra-zinyl)thiazol-5(4H)-one (8d).* Pale yellow crystals; mp 274–276 °C; IR (KBr, cm^{-1}): 3115 (NH), 3066 (CH-aromatic), 2946 (CH aliphatic), 1720 (C=O), 1643 (C=N); ^1H NMR (DMSO- d_6) δ ppm: 3.90 (s, 3H, CH_3), 7.51–7.53 (dd, 2H, Ar-H, J = 8.4 Hz), 7.71–7.72 (m, 2H, Ar-H), 7.93–7.95 (m, 2H, Ar-H), 8.56 (s, 1H, C=CH olefinic), 12.08 (s, 1H, NH, D_2O exchangeable); anal. calcd for $\text{C}_{16}\text{H}_{11}\text{Cl}_2\text{N}_3\text{OS}_2$ (396.3): C, 48.49; H, 2.80; N, 10.60; found: C, 48.34; H, 2.71; N, 10.50%.

4.1.2.c.18. *4-((E)-3,4-Dimethoxybenzylidene)-2-(2-((E)-1-(thiophen-2-yl)ethylidene)hydra-zinyl)thiazol-5(4H)-one (8e).* Buff crystals; mp 248–250 °C; IR (KBr, cm^{-1}): 3122, (NH), 3056 (CH-aromatic), 2943 (CH aliphatic), 1703 (C=O), 1648 (C=N); ^1H NMR (DMSO- d_6) δ ppm: 3.75 (s, 3H, CH_3), 3.84 (s, 6H, OCH_3), 6.97 (d, 2H, Ar-H, J = 8 Hz), 7.07 (s, 1H, Ar-H), 7.14 (d, 2H, Ar-H), 7.53–7.54 (m, 1H, Ar-H), 8.40 (s, 1H, C=CH olefinic), 12.56 (s, 1H, NH, D_2O exchangeable); anal. calcd for $\text{C}_{18}\text{H}_{17}\text{N}_3\text{O}_3\text{S}_2$ (387.5): C, 55.80; H, 4.42; N, 10.84; found: C, 55.66; H, 4.31; N, 10.77%.

4.1.2.c.19. *4-((E)-2,4-Dihydroxybenzylidene)-2-(2-((E)-1-(thiophen-2-yl)ethylidene)hydra-zinyl)thiazol-5(4H)-one (8f).* Red crystals; mp > 300 °C; IR (KBr, cm^{-1}): 3208 (OH, NH), 3092 (CH-aromatic), 2975 (CH aliphatic), 1697 (C=O), 1625 (C=N); ^1H NMR (DMSO- d_6) δ ppm: 3.92 (s, 3H, CH_3), 6.29–6.34 (m, 1H, Ar-H), 6.34–6.36 (dd, 2H,

Ar-H, J = 8.4 Hz), 7.21–7.33 (d, 2H, Ar-H), 8.40 (s, 1H, C=CH olefinic + 1H, Ar-H), 10.07 (s, 1H, NH, for thiazole tautomer D_2O exchangeable), 11.02 (s, 2H, OH, D_2O exchangeable), 11.94 (s, 1H, NH, for thiazole tautomer, D_2O exchangeable); anal. calcd for $\text{C}_{16}\text{H}_{13}\text{N}_3\text{O}_3\text{S}_2$ (359.4): C, 53.47; H, 3.65; N, 11.69; found: C, 53.25; H, 3.53; N, 11.58%.

4.1.2.c.20. *2-(2-((E)-1-(Furan-2-yl)ethylidene)hydra-zinyl)-4-((E)-4-methoxybenzylidene)thiazol-5(4H)-one (8g).* Yellow crystals; mp 288–290 °C; IR (KBr, cm^{-1}): 3434 (NH), 2972 (CH aliphatic), 1722 (C=O), 1634 (C=N), 1602 (C=C); ^1H NMR (DMSO- d_6) δ ppm: 3.83 (s, 3H, CH_3), 3.85 (s, 3H, OCH_3), 6.98–7.01 (m, 3H, Ar-H), 7.66–7.69 (m, 4H, Ar-H), 8.31 (s, 1H, C=CH olefinic), 11.88 (s, 1H, NH, D_2O exchangeable); anal. calcd for $\text{C}_{17}\text{H}_{15}\text{N}_3\text{O}_3\text{S}$ (341.4): C, 59.81; H, 4.43; N, 12.31; found: C, 59.69; H, 4.34; N, 12.20%.

4.1.2.c.21. *4-((E)-4-Chlorobenzylidene)-2-(2-((E)-1-(furan-2-yl)ethylidene)hydra-zinyl)thiazol-5(4H)-one (8h).* Grey crystals; mp 272–274 °C; IR (KBr, cm^{-1}): 3199 (NH), 3027 (CH-aromatic), 2938 (CH aliphatic), 1710 (C=O), 1643 (C=N); ^1H NMR (DMSO- d_6) δ ppm: 3.87 (s, 3H, CH_3), 7.49–7.52 (m, 4H, Ar-H), 7.73–7.80 (m, 3H, Ar-H), 8.39 (s, 1H, C=CH olefinic), 11.97 (s, 1H, NH, D_2O exchangeable); ^{13}C NMR (DMSO- d_6) δ ppm: 162.1, 155.5, 143.1, 142.2, 139.1, 138.0, 136.0, 133.7, 129.6, 129.4, 128.2, 127.4 (2), 111.4, 110.0, 11.3; anal. calcd for $\text{C}_{16}\text{H}_{12}\text{ClN}_3\text{O}_2\text{S}$ (345.8): C, 55.57; H, 3.50; N, 12.15; found: C, 55.35; H, 3.41; N, 12.04%.

4.1.2.c.22. *2-(2-((E)-1-(Furan-2-yl)ethylidene)hydra-zinyl)-4-((E)-4-hydroxybenzylidene)thiazol-5(4H)-one (8i).* Green crystals; mp 293–295 °C; IR (KBr, cm^{-1}): 3238 (OH), 3155 (NH), 3033 (CH-aromatic), 2922 (CH aliphatic), 1689 (C=O), 1639 (C=N); ^1H NMR (DMSO- d_6) δ ppm: 3.81 (s, 3H, CH_3), 6.76–6.82 (m, 4H, Ar-H), 7.55–7.57 (m, 1H, Ar-H), 7.58–7.60 (d, 2H, Ar-H, J = 8 Hz), 8.25 (s, 1H, C=CH olefinic), 9.96 (s, 1H, NH, D_2O exchangeable), 11.82 (s, 1H, OH, D_2O exchangeable); ^{13}C NMR (DMSO- d_6) δ ppm: 160.3, 159.0, 156.8, 151.3, 153.4, 153.1, 149.1, 148.5, 134.3, 129.7(2), 125.5(2), 116.2, 115.6, 11.4; anal. calcd for $\text{C}_{16}\text{H}_{13}\text{N}_3\text{O}_3\text{S}$ (327.4): C, 58.71; H, 4.00; N, 12.84; Found: C, 58.56; H, 3.88; N, 12.71%.

4.1.2.c.23. *4-((E)-2,4-Dichlorobenzylidene)-2-(2-((E)-1-(furan-2-yl)ethylidene)hydra-zinyl)thiazol-5(4H)-one (8j).* White crystals; mp 264–266 °C; IR (KBr, cm^{-1}): 3159 (NH), 3066 (CH-aromatic), 2936 (CH aliphatic), 1720 (C=O), 1644 (C=N); ^1H NMR (DMSO- d_6) δ ppm: 3.91 (s, 3H, CH_3), 7.51–7.53 (dd, 2H, Ar-H, J = 8.4 Hz), 7.72 (d, 1H, Ar-H), 7.93–7.95 (m, 2H, Ar-H), 8.56 (s, 1H, C=CH olefinic + 1H, Ar-H), 12.08 (s, 1H, NH, D_2O exchangeable); anal. calcd for $\text{C}_{16}\text{H}_{11}\text{Cl}_2\text{N}_3\text{O}_2\text{S}$ (380.2): C, 50.54; H, 2.92; N, 11.05; found: C, 50.36; H, 2.81; N, 10.94%.

4.1.2.c.24. *4-((E)-3,4-Dimethoxybenzylidene)-2-(2-((E)-1-(furan-2-yl)ethylidene)hydra-zinyl)thiazol-5(4H)-one (8k).* White crystals; mp 240–242 °C; IR (KBr, cm^{-1}): 3441 (NH), 3088 (CH-aromatic), 2919 (CH aliphatic), 1706 (C=O), 1648 (C=N); ^1H NMR (DMSO- d_6) δ ppm: 3.74 (s, 3H, CH_3), 3.82 (s, 3H, OCH_3), 3.83 (s, 3H, OCH_3), 7.07 (d, 2H, Ar-H, J = 8.4 Hz), 7.27 (m, 3H, Ar-H), 7.51 (m, 1H, Ar-H), 8.29 (s, 1H, C=CH olefinic), 11.91 (s, 1H, NH, D_2O exchangeable), 12.08 (s, 1H, OH, D_2O exchangeable); anal. calcd for $\text{C}_{16}\text{H}_{13}\text{N}_3\text{O}_4\text{S}$ (364.4): C, 53.47; H, 3.65; N, 11.69; found: C, 53.25; H, 3.53; N, 11.58%.



exchangeable); anal. calcd for $C_{18}H_{17}N_3O_4S$ (371.4): C, 58.21; H, 4.61; N, 11.31; found: C, 58.00; H, 4.50; N, 11.40%.

4.1.2.c.25. *4-((E)-2,4-Dihydroxybenzylidene)-2-(2-((E)-1-(furan-2-yl)ethylidene)hydrazinyl)thiazol-5(4H)-one (8l).* Gray crystals; mp 282–284 °C; IR (KBr, cm^{-1}): 3411 (OH), 3150 (NH), 3055 (CH-aromatic), 2952 (CH aliphatic), 1708 (C=O), 1632 (C=N); 1H NMR (DMSO- d_6) δ ppm: 3.92 (s, 3H, CH_3), 6.29–6.34 (m, 1H, Ar-H), 6.34–6.36 (d, 2H, Ar-H, J = 8.4 Hz), 7.31–7.37 (m, 2H, Ar-H), 8.47 (s, 1H, $C=CH$ olefinic + 1H, Ar-H), 10.07 (s, 1H, NH, for thiazole tautomer, D_2O exchangeable), 11.02 (s, 1H, 2OH, D_2O exchangeable), 11.94 (s, 1H, NH, D_2O exchangeable, for thiazole tautomer); anal. calcd for $C_{16}H_{13}N_3O_4S$ (343.4): C, 55.97; H, 3.82; N, 12.24; found: C, 55.77; H, 3.73; N, 12.14%.

4.1.2.c.26. *(E)-2-(2-((E)-1-(Thiophen-2-yl)ethylidene)hydrazinyl)-4-(thiophen-2-ylmethylene)thiazol-5(4H)-one (9a).* Orange crystals; mp 214–216 °C; IR (KBr, cm^{-1}): 3425 (NH), 1717 (C=O), 1635 (C=N); 1H NMR (DMSO- d_6) δ ppm: 3.93 (s, 3H, CH_3), 7.56–7.65 (m, 3H, Ar-H), 7.94–8.08 (dd, 2H, Ar-H), 8.95 (s, 1H, $C=CH$ olefinic H), 9.03 (dd, 1H, Ar-H), 12.03 (s, 1H, NH, D_2O exchangeable); anal. calcd for $C_{14}H_{11}N_3OS_3$ (333.4): C, 50.43; H, 3.33; N, 12.60; found: C, 50.23; H, 3.40; N, 12.51%.

4.1.2.c.27. *(E)-2-(2-((E)-1-(Furan-2-yl)ethylidene)hydrazinyl)-4-(thiophen-2-ylmethylene)thiazol-5(4H)-one (9b).* Yellow crystals; mp 203–205 °C; IR (KBr, cm^{-1}): 3216 (NH), 3091 (CH-aromatic), 2937 (CH aliphatic), 1696 (C=O), 1622 (C=N); 1H NMR (DMSO- d_6) δ ppm: 3.85 (s, 3H, CH_3), 7.12–7.14 (m, 2H, Ar-H), 7.47–7.48 (d, 2H, Ar-H), 7.66–7.67 (d, 2H, Ar-H), 8.53 (s, 1H, $C=CH$ olefinic), 11.90 (s, 1H, NH, D_2O exchangeable); anal. calcd for $C_{14}H_{11}N_3O_2S_2$ (317.4): C, 52.98; H, 3.49; N, 13.24; found: C, 52.77; H, 3.37; N, 13.13%.

4.2. Biological evaluation

4.2.1. *In vitro* cytotoxic activity. Evaluation of cytotoxic activity of the synthesized compounds was carried out using MTT assay protocol^{49,50,57} against a group of cancer cell lines namely; colorectal carcinoma (HCT-116), Hepatocellular carcinoma (HepG-2) and breast cancer (MCF-7) and colchicine was used as a standard drug. The cells were obtained from ATCC (American Type Culture Collection) via the Holding company for biological products and vaccines (VACSER) (Cairo, Egypt). The anti-cancer activity was measured quantitatively as follows:

Into a medium of RPMI-1640 with 10% fetal bovine serum, the cell lines were cultured. Then, penicillin (100 units per mL) and streptomycin (100 μ g mL⁻¹) were added at 37 °C in a 5% CO₂ incubator. Next, seeding the cell lines in a 96-well plate was achieved by a density of 1.0×10^4 cells per well at 37 °C for 48 h under 5% CO₂. After incubation period, the cell lines were treated with different concentration of the synthesized compounds and incubated for 24 h. After treatment by 24 h, 20 μ L of MTT solution (5 mg mL⁻¹) was added and incubated for 4 h. Dimethyl sulfoxide (100 μ L) was added into each well to dissolve the formed purple formazan. The colorimetric assay was measured and recorded at absorbance of 570 nm using a plate reader (EXL 800, USA). The relative cell viability in percentage was calculated as (A570 of treated samples/A570 of

untreated sample) \times 100. Results for IC₅₀ values of the active compounds were summarized in Table 1.

4.2.2. *In vitro* tubulin polymerization assay. The effect of the synthesized compounds on tubulin polymerization was assessed turbidimetrically using a fluorescent plate reader method.⁵² At first, the synthesized compounds and reference drug (colchicine) were incubated in mixture of purified bovine tubulin (10 μ M) and buffer system containing 20% glycerol and 1 mM ATP at 37 °C. Then, the mixture cooled to 0 °C. The IC₅₀ value was defined as the compound concentration that inhibited the extent of tubulin assembly by 50%.

4.2.3. Cell cycle analysis. HepG-2 cells were seeded at density of 2×10^5 cells per well and incubated for 24 h in six-well plates. Fetal bovine serum (FBS, 10%) was added, after that cells were incubated at 37 °C and 5% CO₂. The medium was replaced with (DMSO 1% v/v) containing the 2.5 μ M of compound 5a, then incubated for 48 h, washed with cold phosphate buffered saline (PBS), fixed with 70% ethanol, rinsed with PBS then stained with the DNA fluorochrome PI, kept for 15 min at 37 °C. Then samples were analyzed with a FACS Caliber flow cytometer.⁵³

4.2.4. Annexin V-FITC apoptosis assay. The effect of the most cytotoxic compound 5a on apoptosis induction was analyzed using Annexin V-FITC/PI apoptosis detection kit. In this test, HepG-2 cells were stained with Annexin V fluorescein isothiocyanate (FITC) and counterstained with propidium iodide (PI). Then, HepG-2 cells in a density of 2×10^5 per well were incubated with compound 5a for 48 h. Next, the cells were trypsinized, washed with phosphate-buffered saline (PBS), and stained for 15 min at 37 °C in the dark. Finally, FACS Caliber flow cytometer was used in analysis process.⁵⁵

4.3. Docking studies

Crystallographic structure of tubulin [PDB ID: 1SA0, resolution 3.00 Å] was retrieved from Protein Data Bank (<http://www.pdb.org>) and considered as a target for docking simulation. The docking analysis was performed using MOE2014 software to evaluate the free energy and binding modes of the synthesized compounds against tubulin. At first, the crystal structure of the target was prepared by removing water molecules and retaining the two essential chains and the co-crystallized ligand, *N*-deacetyl-*N*-(2-mercaptoacetyl)-colchicine (DAMA-colchicine). Then, the protein structure was protonated, and the hydrogen atoms were added. Next, the energy was minimized, and the binding pocket of the protein was defined.

The 2D structures of the synthesized compounds and reference ligand (DAMA-colchicine) were sketched using ChemBioDraw Ultra 14.0 and saved as MDL-SD format. Then, the saved files were opened using MOE and 3D structures were protonated. Next, energy minimization was applied. Before docking process, validation of the docking protocol was carried out by running the simulation only using the co-crystallized ligand (DAMA-colchicine) which showed low RMSD value. The molecular docking of the synthesized was performed using a default protocol against the target receptor. In each case, 30 docked structures were generated using genetic algorithm



searches, London dG was used for scoring and forcefield (MMFF94) for refinement. The London dG scoring function estimates the free energy of binding of the ligand from a given pose. The functional form is a sum of terms:

$$\Delta G = c + E_{\text{flex}} + \sum_{\text{h-bonds}} c_{\text{HB}} f_{\text{HB}} + \sum_{\text{m-lig}} c_{\text{M}} f_{\text{M}} + \sum_{\text{atom i}} \Delta D_i$$

where C represents the average gain/loss of rotational and translational entropy; E_{flex} is the energy due to the loss of flexibility of the ligand (calculated from ligand topology only); f_{HB} measures geometric imperfections of hydrogen bonds and takes a value in $[0,1]$; c_{HB} is the energy of an ideal hydrogen bond; f_{M} measures geometric imperfections of metal ligations and takes a value in $[0,1]$; c_{M} is the energy of an ideal metal ligation; and D_i is the desolvation energy of atom i .

The output from of MOE was further analyzed and visualized using Discovery Studio 4.0 software.^{58–61}

Conflicts of interest

This work was funded by the authors and there is no any conflict of interest.

References

1. S. Mukherjee, *The emperor of all maladies: a biography of cancer*, Simon and Schuster, 2010.
2. C. Holohan, S. Van Schaeybroeck, D. B. Longley and P. G. Johnston, Cancer drug resistance: an evolving paradigm, *Nat. Rev. Cancer*, 2013, **13**, 714.
3. H. Zahreddine and K. Borden, Mechanisms and insights into drug resistance in cancer, *Front. Pharmacol.*, 2013, **4**, 28.
4. M.-F. Chau, M. J. Radeke, C. de Inés, I. Barasoain, L. A. Kohlstaedt and S. C. Feinstein, The microtubule-associated protein tau cross-links to two distinct sites on each α and β tubulin monomer via separate domains, *Biochem.*, 1998, **37**, 17692–17703.
5. S. Honore, E. Pasquier and D. Braguer, Understanding microtubule dynamics for improved cancer therapy, *Cell Mol. Life Sci.*, 2005, **62**, 3039–3056.
6. D. A. Fletcher and R. D. Mullins, Cell mechanics and the cytoskeleton, *Nature*, 2010, **463**, 485.
7. E. A. Nigg, Cell division: mitotic kinases as regulators of cell division and its checkpoints, *Nat. Rev. Mol. Cell Biol.*, 2001, **2**, 21.
8. J. J. Field, A. Kanakkanthara and J. H. Miller, Microtubule-targeting agents are clinically successful due to both mitotic and interphase impairment of microtubule function, *Bioorg. Med. Chem.*, 2014, **22**, 5050–5059.
9. L. Wilson and M. A. Jordan, Microtubule dynamics: taking aim at a moving target, *Chem. Biol.*, 1995, **2**, 569–573.
10. K. Haider, S. Rahaman, M. S. Yar and K. Ahmed, Tubulin inhibitors as novel anticancer agents: an overview on patents (2013–2018), *Expert Opin. Ther. Pat.*, 2019, **29**(8), 623–641, DOI: 10.1080/13543776.2019.1648433.
11. M. Botta, S. Forli, M. Magnani, F. Manetti, Molecular modeling approaches to study the binding mode on tubulin of microtubule destabilizing and stabilizing agents, in *Tubulin-Binding Agents*, Springer, 2008, pp. 279–328.
12. R. Altaha, T. Fojo, E. Reed and J. Abraham, Epothilones: a novel class of non-taxane microtubule-stabilizing agents, *Curr. Pharm. Des.*, 2002, **8**, 1707–1712.
13. A. E. Prota, K. Bargsten, J. F. Diaz, M. Marsh, C. Cuevas, M. Liniger, C. Neuhaus, J. M. Andreu, K.-H. Altmann and M. O. Steinmetz, A new tubulin-binding site and pharmacophore for microtubule-destabilizing anticancer drugs, *Proc. Natl. Acad. Sci. U. S. A.*, 2014, **111**, 13817–13821.
14. Y. Lu, J. Chen, M. Xiao, W. Li and D. D. Miller, An overview of tubulin inhibitors that interact with the colchicine binding site, *Pharm. Res.*, 2012, **29**, 2943–2971.
15. L. Li, S. Jiang, X. Li, Y. Liu, J. Su and J. Chen, Recent advances in trimethoxyphenyl (TMP) based tubulin inhibitors targeting the colchicine binding site, *Eur. J. Med. Chem.*, 2018, **151**, 482–494.
16. J. Zhou and P. Giannakakou, Targeting microtubules for cancer chemotherapy, *Curr. Med. Chem.*, 2005, **5**, 65–71.
17. G. R. Pettit, J. W. Lippert, D. L. Herald, E. Hamel and R. K. Pettit, Antineoplastic Agents 440. Asymmetric Synthesis and Evaluation of the Combretastatin A-1 SAR Probes (1 S, 2 S)-and (1 R, 2 R)-1, 2-Dihydroxy-1-(2', 3'-dihydroxy-4'-methoxyphenyl)-2-(3", 4", 5"-trimethoxyphenyl)-ethane, *J. Nat. Prod.*, 2000, **63**, 969–974.
18. G. R. Pettit and J. W. Lippert, Antineoplastic agents 429. Syntheses of the combretastatin A-1 and combretastatin B-1 prodrugs, *Anti-Cancer Drug Des.*, 2000, **15**, 203–216.
19. G. R. Pettit, J. C. Temple, V. Narayanan, R. Varma, M. Simpson, M. Boyd, G. Rener and N. Bansal, Antineoplastic agents 322. synthesis of combretastatin A-4 prodrugs, *Anti-Cancer Drug Des.*, 1995, **10**, 299–309.
20. I. G. Kirwan, P. M. Loadman, D. J. Swaine, D. A. Anthoney, G. R. Pettit, J. W. Lippert, S. D. Shnyder, P. A. Cooper and M. C. Bibby, Comparative preclinical pharmacokinetic and metabolic studies of the combretastatin prodrugs combretastatin A4 phosphate and A1 phosphate, *Clin. Cancer Res.*, 2004, **10**, 1446–1453.
21. S. A. Horner, S. Gould, J. P. Noakes, N. J. Rattray, S. L. Allen, E. Zotova and J. C. Arezzo, Lack of neurotoxicity of the vascular targeting agent ZD6126 following repeated iv dosing in the rat, *Mol. Cancer Ther.*, 2004, **3**, 783–791.
22. H. Goto, S. Yano, H. Zhang, Y. Matsumori, H. Ogawa, D. C. Blakey and S. Sone, Activity of a new vascular targeting agent, ZD6126, in pulmonary metastases by human lung adenocarcinoma in nude mice, *Cancer Res.*, 2002, **62**, 3711–3715.
23. K. R. Hande, A. Hagey, J. Berlin, Y. Cai, K. Meek, H. Kobayashi, A. C. Lockhart, D. Medina, J. Sosman and G. B. Gordon, The pharmacokinetics and safety of ABT-751, a novel, orally bioavailable sulfonamide antimitotic agent: results of a phase 1 study, *Clin. Cancer Res.*, 2006, **12**, 2834–2840.
24. Z. Ding, H. Cheng, S. Wang, Y. Hou, J. Zhao, H. Guan and W. Li, Development of MBRI-001, a deuterium-substituted



plinabulin derivative as a potent anti-cancer agent, *Bioorg. Med. Chem. Lett.*, 2017, **27**, 1416–1419.

25 G. K. Lloyd, P. Mueller, A. Zippelius and L. Huang, Abstract A07: Plinabulin: Evidence for an immune-mediated mechanism of action, *Cancer Res.*, 2016, **76**, A07.

26 A. V. Singh, M. Bandi, N. Raje, P. Richardson, M. A. Palladino, D. Chauhan and K. C. Anderson, A novel vascular disrupting agent plinabulin triggers JNK-mediated apoptosis and inhibits angiogenesis in multiple myeloma cells, *Blood*, 2011, **117**, 5692–5700.

27 S. Kapoor, S. Srivastava and D. Panda, Indibulin dampens microtubule dynamics and produces synergistic antiproliferative effect with vinblastine in MCF-7 cells: Implications in cancer chemotherapy, *Sci. Rep.*, 2018, **8**, 12363.

28 G. Bacher, B. Nickel, P. Emig, U. Vanhoefer, S. Seeber, A. Shandra, T. Klenner and T. Beckers, D-24851, a novel synthetic microtubule inhibitor, exerts curative antitumoral activity *in vivo*, shows efficacy toward multidrug-resistant tumor cells, and lacks neurotoxicity, *Cancer Res.*, 2001, **61**, 392–399.

29 M. P. Tantak, L. Klingler, V. Arun, A. Kumar, R. Sadana and D. Kumar, Design and synthesis of bis (indolyl) ketohydrazide-hydrazone: Identification of potent and selective novel tubulin inhibitors, *Eur. J. Med. Chem.*, 2017, **136**, 184–194.

30 Y. Lu, J. Chen, J. Wang, C.-M. Li, S. Ahn, C. M. Barrett, J. T. Dalton, W. Li and D. D. Miller, Design, synthesis, and biological evaluation of stable colchicine binding site tubulin inhibitors as potential anticancer agents, *J. Med. Chem.*, 2014, **57**, 7355–7366.

31 A. Tripathi, D. Durrant, R. M. Lee, R. Baruchello, R. Romagnoli, D. Simoni and G. E. Kellogg, Hydropathic analysis and biological evaluation of stilbene derivatives as colchicine site microtubule inhibitors with anti-leukemic activity, *J. Enzyme Inhib. Med. Chem.*, 2009, **24**, 1237–1244.

32 T. L. Nguyen, C. McGrath, A. R. Hermone, J. C. Burnett, D. W. Zaharevitz, B. W. Day, P. Wipf, E. Hamel and R. Gussio, A common pharmacophore for a diverse set of colchicine site inhibitors using a structure-based approach, *J. Med. Chem.*, 2005, **48**, 6107–6116.

33 B. Bhattacharyya, D. Panda, S. Gupta and M. Banerjee, Anti-mitotic activity of colchicine and the structural basis for its interaction with tubulin, *Med. Res. Rev.*, 2008, **28**, 155–183.

34 D. Simoni, G. Grisolia, G. Giannini, M. Roberti, R. Rondanin, L. Piccagli, R. Baruchello, M. Rossi, R. Romagnoli and F. P. Invidiata, Heterocyclic and phenyl double-bond-locked combretastatin analogues possessing potent apoptosis-inducing activity in HL60 and in MDR cell lines, *J. Med. Chem.*, 2005, **48**, 723–736.

35 H. A. Mahdy, M. K. Ibrahim, A. M. Metwaly, A. Belal, A. B. Mehany, A. El-Sharkawy, M. A. Elhendawy, M. M. Radwan, M. A. Elsohly and I. H. Eissa, Design, synthesis, molecular modeling, *in vivo* studies and anticancer evaluation of quinazolin-4 (3H)-one derivatives as potential VEGFR-2 inhibitors and apoptosis inducers, *Bioorg. Chem.*, 2019, 103422.

36 A. G. A. El-Helby, H. Sakr, I. H. Eissa, A. A. Al-Karmalawy and K. El-Adl, Benzoxazole/benzothiazole-derived VEGFR-2 inhibitors: Design, synthesis, molecular docking, and anticancer evaluations, *Arch. Pharm.*, 2019, e1900178.

37 I. H. Eissa, A. M. Metwaly, A. Belal, A. B. Mehany, R. R. Ayyad, K. El-Adl, H. A. Mahdy, M. S. Taghour, K. M. El-Gamal and M. E. El-Sawah, Discovery and antiproliferative evaluation of new quinoxalines as potential DNA intercalators and topoisomerase II inhibitors, *Arch. Pharm.*, 2019, e1900123.

38 A. G. A. El-Helby, H. Sakr, I. H. Eissa, H. Abulkhair, A. A. Al-Karmalawy and K. El-Adl, Design, synthesis, molecular docking, and anticancer activity of benzoxazole derivatives as VEGFR-2 inhibitors, *Arch. Pharm.*, 2019, **352**, 1900113.

39 S. A. Elmetwally, K. F. Saied, I. H. Eissa and E. B. Elkaeed, Design, synthesis and anticancer evaluation of thieno [2, 3-d] pyrimidine derivatives as dual EGFR/HER2 inhibitors and apoptosis inducers, *Bioorg. Chem.*, 2019, **88**, 102944.

40 M. Ibrahim, M. Taghour, A. Metwaly, A. Belal, A. Mehany, M. Elhendawy, M. Radwan, A. Yassin, N. El-Deeb and E. Hafez, Design, synthesis, molecular modeling and anti-proliferative evaluation of novel quinoxaline derivatives as potential DNA intercalators and topoisomerase II inhibitors, *Eur. J. Med. Chem.*, 2018, **155**, 117–134.

41 A. A. Gaber, A. H. Bayoumi, A. M. El-morsy, F. F. Sherbiny, A. B. Mehany and I. H. Eissa, Design, synthesis and anticancer evaluation of 1H-pyrazolo [3, 4-d] pyrimidine derivatives as potent EGFRWT and EGFR790M inhibitors and apoptosis inducers, *Bioorg. Chem.*, 2018, **80**, 375–395.

42 I. H. Eissa, A. M. El-Naggar, N. E. El-Sattar and A. S. Youssef, Design and discovery of novel quinoxaline derivatives as dual DNA intercalators and topoisomerase II inhibitors, *Anti-Cancer Agents Med. Chem.*, 2018, **18**, 195–209.

43 A. M. El-Naggar, M. M. Abou-El-Regal, S. A. El-Metwally, F. F. Sherbiny and I. H. Eissa, Synthesis, characterization and molecular docking studies of thiouracil derivatives as potent thymidylate synthase inhibitors and potential anticancer agents, *Mol. Divers.*, 2017, **21**, 967–983.

44 W. M. Eldehna, M. F. Abo-Ashour, A. Nocentini, P. Gratteri, I. H. Eissa, M. Fares, O. E. Ismael, H. A. Ghabbour, M. M. Elaasser and H. A. Abdel-Aziz, Novel 4/3-((4-oxo-5-(2-oxoindolin-3-ylidene) thiazolidin-2-ylidene) amino) benzenesulfonamides: Synthesis, carbonic anhydrase inhibitory activity, anticancer activity and molecular modelling studies, *Eur. J. Med. Chem.*, 2017, **139**, 250–262.

45 I. H. Eissa, A. M. El-Naggar and M. A. El-Hashash, Design, synthesis, molecular modeling and biological evaluation of novel 1H-pyrazolo [3, 4-b] pyridine derivatives as potential anticancer agents, *Bioorg. Chem.*, 2016, **67**, 43–56.

46 A. M. El-Naggar, M. M. Hemdan and S. R. Atta-Allah, An Efficient One-Pot Synthesis of New Coumarin Derivatives as Potent Anticancer Agents under Microwave Irradiation, *J. Heterocycl. Chem.*, 2017, **54**, 3519–3526.

47 A. M. El-Naggar, A. K. Khalil, H. M. Zeidan and W. M. El-Sayed, Eco-friendly Synthesis of Pyrido [2, 3-d] pyrimidine



Analogs and Their Anticancer and Tyrosine Kinase Inhibition Activities, *Anti-Cancer Agents Med. Chem.*, 2017, **17**, 1644–1651.

48 K. A. Abouzid, G. H. Al-Ansary and A. M. El-Naggar, Eco-friendly synthesis of novel cyanopyridine derivatives and their anticancer and PIM-1 kinase inhibitory activities, *Eur. J. Med. Chem.*, 2017, **134**, 357–365.

49 T. Mosmann, Rapid colorimetric assay for cellular growth and survival: application to proliferation and cytotoxicity assays, *J. Immunol. Methods*, 1983, **65**, 55–63.

50 F. Denizot and R. Lang, Rapid colorimetric assay for cell growth and survival: modifications to the tetrazolium dye procedure giving improved sensitivity and reliability, *J. Immunol. Methods*, 1986, **89**, 271–277.

51 M. Thabrew, R. D. Hughes and I. G. Mcfarlane, Screening of hepatoprotective plant components using a HepG2 cell cytotoxicity assay, *J. Pharm. Pharmacol.*, 1997, **49**, 1132–1135.

52 G. M. Morris, D. S. Goodsell, R. S. Halliday, R. Huey, W. E. Hart, R. K. Belew and A. J. Olson, Automated docking using a Lamarckian genetic algorithm and an empirical binding free energy function, *J. Comput. Chem.*, 1998, **19**, 1639–1662.

53 J. Wang and M. J. Lenardo, Roles of caspases in apoptosis, development, and cytokine maturation revealed by homozygous gene deficiencies, *J. Cell Sci.*, 2000, **113**, 753–757.

54 J. M. Brown and B. G. Wouters, Apoptosis, p53, and tumor cell sensitivity to anticancer agents, *Cancer Res.*, 1999, **59**, 1391–1399.

55 K. K.-W. Lo, T. K.-M. Lee, J. S.-Y. Lau, W.-L. Poon and S.-H. Cheng, Luminescent biological probes derived from ruthenium (II) estradiol polypyridine complexes, *Inorg. Chem.*, 2008, **47**, 200–208.

56 A. G. A. El-Helby, R. R. Ayyad, H. M. Sakr, A. S. Abdelrahim, K. El-Adl, F. S. Sherbiny, I. H. Eissa and M. M. Khalifa, Design, synthesis, molecular modeling and biological evaluation of novel 2, 3-dihydropthalazine-1, 4-dione derivatives as potential anticonvulsant agents, *J. Mol. Struct.*, 2017, **1130**, 333–351.

57 M. I. Thabrew, R. D. Hughes and I. G. Mcfarlane, Screening of hepatoprotective plant components using a HepG2 cell cytotoxicity assay, *J. Pharm. Pharmacol.*, 1997, **49**, 1132–1135.

58 M. A. El-Zahabi, E. R. Elbendary, F. H. Bamanie, M. F. Radwan, S. A. Ghareib and I. H. Eissa, Design, synthesis, molecular modeling and anti-hyperglycemic evaluation of phthalimide-sulfonylurea hybrids as PPAR γ and SUR agonists, *Bioorg. Chem.*, 2019, **91**, 103115.

59 M. K. Ibrahim, I. H. Eissa, M. S. Alesawy, A. M. Metwaly, M. M. Radwan and M. A. ElSohly, Design, synthesis, molecular modeling and anti-hyperglycemic evaluation of quinazolin-4 (3H)-one derivatives as potential PPAR γ and SUR agonists, *Bioorg. Med. Chem.*, 2017, **25**, 4723–4744.

60 M. K. Ibrahim, I. H. Eissa, A. E. Abdallah, A. M. Metwaly, M. Radwan and M. ElSohly, Design, synthesis, molecular modeling and anti-hyperglycemic evaluation of novel quinoxaline derivatives as potential PPAR γ and SUR agonists, *Bioorg. Med. Chem.*, 2017, **25**, 1496–1513.

61 K. M. El-Gamal, A. M. El-Morsy, A. M. Saad, I. H. Eissa and M. Alswah, Synthesis, docking, QSAR, ADMET and antimicrobial evaluation of new quinoline-3-carbonitrile derivatives as potential DNA-gyrase inhibitors, *J. Mol. Struct.*, 2018, **1166**, 15–33.

